Neurobiology of Stress 31 (2024) 100654

Contents lists available at ScienceDirect

Neurobiology of Stress

journal homepage: www.elsevier.com/locate/ynstr

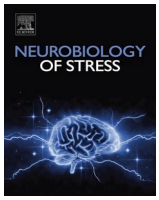

Hyperexcitation of the glutamatergic neurons in lateral hypothalamus induced by chronic pain contributes to depression-like behavior and learning and memory impairment in male mice

Lianghui Meng [1], Xuefeng Zheng [1], Keman Xie, Yifei Li, Danlei Liu, Yuanyuan Xu, Jifeng Zhang [**], Fengming Wu [***], Guoqing Guo [*]

Department of Anatomy, Neuroscience Laboratory for Cognitive and Developmental Disorders, Medical College of Jinan University, Guangzhou, 510630, China

ARTICLE INFO

Handling Editor: Prof R Lawrence Reagan

Keywords:
Chronic pain
Lateral hypothalamus
Glutamatergic neurons
Depression-like behavior
Learning and memory impairment

ABSTRACT

Chronic pain can induce mood disorders and cognitive dysfunctions, such as anxiety, depression, and learning and memory impairment in humans. However, the specific neural network involved in anxiety- and depression-like behaviors and learning and memory impairment caused by chronic pain remains poorly understood. In this study, behavioral test results showed that chronic pain induced anxiety- and depression-like behaviors, and learning and memory impairment in male mice. c-Fos immunofluorescence and fiber photometry recording showed that glutamatergic neurons in the LH of mice with chronic pain were selectively activated. Next, the glutamatergic neurons of LH in normal mice were activated using optogenetic and chemogenetic methods, which recapitulates some of the depressive-like behaviors, as well as memory impairment, but not anxiety-like behavior. Finally, inhibition of glutamatergic neurons in the LH of mice with chronic pain, effectively relieved anxiety- and depression-like behaviors and learning and memory impairment. Taken together, our findings suggest that hyperexcitation of glutamatergic neurons in the LH is involved in depression-like behavior and learning and memory impairment induced by chronic pain.

1. Introduction

Pain is protective and warns against tissue damage; therefore, it is essential for survival (Donnelly et al., 2020). However, chronic pain is a persistent and inescapable experience that leads to maladaptive emotional states (Gilam et al., 2020). In addition to unpleasant sensations, patients with chronic pain are often accompanied with emotional disorders. Chronic pain is a serious health problem that affects many patients. Clinical surveys have revealed that 30–60% of patients with chronic pain experience severe depression or anxiety (Ma et al., 2021; Tappe-Theodor and Kuner, 2019). Moreover, patients with chronic pain often report impaired cognitive functions, including deficits in attention, memory, executive planning, and information processing (Zhang et al., 2021). The emergence of various adverse emotions and cognitive dysfunction after chronic pain reduces patients' quality of life. In particular, emotional disorders may lead to excessive duration and intensity of pain (Bonilla-Jaime et al., 2022). This creates a vicious cycle of pain and emotional disorders. Thus, the management of mood and cognitive disorders in chronic pain is challenging and lies in understanding the neurological, structural, and functional bases of comorbidities.

The hypothalamus is responsible for maintaining homeostatic balance in physiology and behavior by integrating vast amounts of neural and humoral information and conveying appropriate instructions to downstream brain regions (Tran et al., 2022). Clinical neuroimaging studies have demonstrated that hypothalamic activity change were found in both pain patients and depression patients (Schindler et al., 2019; Sprenger et al., 2005). Hypothalamus is mainly composed of the medial preoptic area (MPO), paraventricular nucleus of hypothalamus (PVN), anterior hypothalamic nucleus (AHN), lateral hypothalamus (LH), ventromedial hypothalamus (VMH), dorsomedial hypothalamus (DMH), arcuate nucleus (Arc), and supramammillary nucleus (SUM),

* Corresponding author.
** Corresponding author.
*** Corresponding author.
E-mail addresses: tzjf_jennifer@jnu.edu.cn (J. Zhang), twufengming@jnu.edu.cn (F. Wu), tgqguo@jnu.edu.cn (G. Guo).
[1] These authors contributed equally: Lianghui Meng, Xuefeng Zheng.

https://doi.org/10.1016/j.ynstr.2024.100654
Received 17 October 2023; Received in revised form 29 May 2024; Accepted 30 May 2024
Available online 1 June 2024

which are related to mood disorders (Daviu et al., 2020; Jia et al., 2022; Li et al., 2022, 2023; Shin et al., 2023; Tang et al., 2022; Wang et al., 2023; Wang et al., 2023, 2023; Yan et al., 2022). Animal studies have shown that the LH plays a key role in regulating wakefulness, sleep, food intake, autonomic and endocrine functions, reward-related behavior, anxiety-and depression-like behaviors, and learning and memory (Bonnavion et al., 2016; Gu et al., 2023; Tang et al., 2022). The LH function relies on the differentiated neurons, most of which are glutamatergic or GABAergic (Zhou et al., 2021). The activity of glutamatergic neurons in the LH was selectively elevated in mice experiencing chronic pain. (Gu et al., 2023), suggesting that the LH may be involved in the pathological process of chronic pain or the behavioral abnormalities induced by chronic pain.

This study aimed to illustrate the role of LH in mood disorders and cognitive dysfunction following chronic pain induced by spared nerve injury (SNI). First, we confirmed that chronic pain induces anxiety- and depression-like behaviors as well as learning and memory dysfunction, accompanied by strong activation of glutamatergic neurons in the LH. Furthermore, chemogenetic and optogenetic activation of glutamatergic neurons in the LH results in depression-like behavior and learning and memory impairment in normal mice, but not anxiety-like behavior. Finally, chemogenetic inhibition of glutamatergic neurons in the LH significantly rescued SNI-induced anxiety- and depression-like behaviors and learning and memory impairment in mice. Altogether, our findings revealed that glutamatergic neurons in the LH play a crucial role in the generation of depression-like behavior and learning and memory impairment after chronic pain.

2. Materials and methods

2.1. Animals

All animal experiments were conducted in accordance with the National Institutes of Health Guidelines for the Care and Use of Laboratory Animals, and were approved by the Laboratory Animal Ethics Committee of Jinan University (Guangzhou, China) in accordance with the experimental animal management regulations. Male C57BL/6J mice (8 weeks old, 20–24 g body weight) were purchased from Liaoning Changsheng Biotechnology Company. 5–6 mice of the same group were housed per cage. They were housed at a constant temperature (20–25 °C) and humidity (40–60%) in a controlled facility on a 12 h light/dark cycle (light from 8:00 to 20:00) with food and water ad libitum. The mice were acclimated to the room for one week prior to the experiments.

2.2. Chronic pain model

The SNI surgery was performed as previously described (Decosterd and Woolf, 2000). Mice were anesthetized with 1% isoflurane and fixed to an operating table: one end of the thread is secured to each limb of the mouse, while the other end is anchored to each corner of the operating table, so that the body of mouse is fully extended. Then, an 0.5-cm length skin incision was made on the left thigh, and the skin and muscles of the left thigh were separated via blunt resection to explore the three branches of the sciatic nerve, including the sural, common peroneal, and tibial nerves. After using 5-0 silk sutures to ligate the tibial and common peroneal nerves, they were completely transected distal to the ligation sites, a 1-mm piece of the nerves was removed. Precaution was taken to avoid damage to the sural nerve. Finally, the muscle and skin were separately sutured using 4-0 silk sutures and disinfected using iodophor. In the sham group, the same procedure was performed without nerve ligation and transection of the nerves. After surgery, the mice were placed in a warm chamber for 30 min.

2.3. The von Frey test

The mechanical paw withdrawal (PW) threshold was assessed using an electronic von Frey aesthesiometer with flexible von Frey hair (NJKEWBIO, China) (Wang et al., 2020). Before each test, the von Frey hair was connected to the electronic system to record the results. The mice were placed in a test Plexiglas cage on an elevated mesh floor for at least 40 min for habituation. The lateral plantar region (innervated by the sural nerve) was stimulated by the von Frey hair. The minimum force required to retract their hind legs or lick their hind feet was recorded. Three trials of withdrawal per paw with a 10 min interval between tests were recorded, and an average was calculated. Mechanical PW thresholds were measured the day before surgery and once a week after surgery.

2.4. Behavioral tests

Behavioral tests were performed after the SNI modeling or virus injection. All behavioral tests were conducted during the light cycle. The mice were acclimatized to the test environment for 45 min before each behavioral test. The laboratory apparatus was cleaned with 75% alcohol between each test and the behavior of the mice was automatically analyzed using a behavior analysis system (Topscanlite 3.0).

2.4.1. Open field test (OFT)

The OFT was used to measure anxiety-like behavior (Kraeuter et al., 2019a). Briefly, the mice were gently removed from the home cage and placed in the center of an open-field arena (40 cm length × 40 cm width × 40 cm height). The arena was brightly lit (1100–1200 lux). The mice were allowed to freely explore the arena for 10 min. The motion trials were recorded using a camera directly above the arena. The time spent in the central area and the total distance moved were counted.

2.4.2. Elevated plus maze (EPM)

Anxiety level was also assessed using the elevated plus maze (EPM) test, as previously described (Kraeuter et al., 2019b). The maze consisted of four elevated arms (35 cm length × 5 cm width) that intersected at right angles. Two opposite arms were enclosed by 15 cm high walls, and the other two were open (no walls). The whole maze was elevated 60 cm above the ground, and the mice were placed at the 5 cm × 5 cm intersection of the maze facing an arm without walls to start a trial. The amount of time the mice spent in the open arms and the number of entries into open and close arms throughout a 10-min session were calculated.

2.4.3. Forced swimming test (FST)

The forced swimming test (FST) has been used to assess depression-like behavior (Yankelevitch-Yahav et al., 2015). The cylindrical tanks (28 cm height × 16 cm diameter) used in the mice forced swimming test were constructed of transparent Plexiglas. Then mice were held by the tail and gently placed in the tanks with about 20 cm of water (23–25 °C) for 6 min. Before each test, the water was changed to prevent the influence of pheromones left behind by the previous mice. Locomotion was recorded from the side using a camera. The mice were considered immobile when they were floating without any other movement, and the immobility time in the last 4 min was measured with the behavior analyzing system (Topscanlite 3.0). After the test, the mice were dried and returned to their home cages.

2.4.4. Tail suspension test (TST)

To assess depression-like behavior, the mice were subjected to a tail suspension test (TST) as previously described (Cryan et al., 2005). They were suspended in a box (20 cm length × 20 cm width × 30 cm height) by wrapping tape approximately 1 cm from the tail tip and 30 cm above the ground. The entire suspension lasted for 6 min and the immobility time in the last 4 min was recorded. All the tests were recorded by a

video camera and analyzed using a behavior analyzing system (Topscanlite 3.0).

2.4.5. Novelty suppression feeding test (NSF)

To assess depression-like behavior, mice were subjected to a novelty suppression feeding test (NSF) as previously described (Cui et al., 2022). The test apparatus comprised a plastic box (50 cm length × 50 cm width × 20 cm height). The floor was covered with approximately 2 cm of corn cob bedding, and the arena was brightly lit (1100–1200 lux). The mice were fasted for 24 h. At the time of testing, they were placed in the corner of the box with a single pellet of food (regular chow) placed on a white paper platform positioned in the center. The time to the first chewing of the food (lantency) was recorded. The test lasted for 10 min and if the mice had not eaten the latency was scored as 10 min. Immediately after latency was recorded, the food pellet was removed from the arena. The mice were then placed in home cages and the time to the first chewing of the food (latency) was recorded. The test lasted for 10 min and if the mice had not eaten the latency was scored as 10 min.

2.4.6. Sucrose splash test (SST)

The sucrose splash test (SST) was conducted to assess depression-like behavior (Dai et al., 2022). The mice were placed in an unfamiliar white plastic box (40 cm length × 30 cm width × 20 cm height). Before testing, they were allowed to explore freely for 1 min. At the time of testing, the backs of the mice were sprayed with 10% sucrose solution. The test lasted for 5 min and the total grooming time was recorded.

2.4.7. Y maze

The Y maze test was used to assess spatial recognition memory in mice (Kraeuter et al., 2019c). The luminance of overhead white lighting is 40 lux and markers were placed on the walls in each of the four directions within the room. These markers were characterized by distinct colors contrasting with the wall background (e.g., circle, square, pentagon, triangle). The Y maze consisted of three arms (40 cm length × 5 cm width × 10 cm height) at a 120° angle from each other. The experiments were divided into two phases. In the learning phase, the mice were placed at the end of one arm (designated as the start arm). Only two arms were open (the familiar arm), and the third arm was blocked (the novel arm). The mice were allowed to explore freely in the start and familiar arms for 10 min. After a 2 h inter-trial interval, the testing phase began with the novel arm opening and the mice were put back at the end of the start arm for 3 min to explore, with free access to all three arms. The choices of novel and familiar arms alternated between the tests for different subjects. The trials were recorded using a camera and analyzed using a behavior analyzing system (Topscanlite 3.0). The percentage of time mice spent in the novel arm relative to the total time was analyzed.

2.4.8. Morris water maze (MWM)

We used the Morris water maze (MWM) test to evaluate spatial learning and memory abilities (Othman et al., 2022). Briefly, a circular pool (120 cm in diameter, 45 cm in depth) was filled with water (maintained at 25 °C) that contained titanium dioxide (T164497, Biohonor, China) to make it opaque in a dimly lit room. Two principal axes perpendicular to each other were designated to create an imaginary "+", and the pool was divided into four equal quadrants. The intersection points of the axes with the pool edge were designated north (N), south (S), east (E), and west (W). Conspicuous markers were placed on the walls in each of the four directions within the room. These markers were characterized by distinct colors contrasting with the wall background (e.g., circle, square, pentagon, triangle). A circular platform (10 cm in diameter and 1 cm underwater) was placed in a fixed quadrant. The experiment lasted for six days. The first five days were the learning phase and the sixth day was the testing phase. In the learning phase, the mice were given 3 trials (90 s each) per day, with an inter-trial interval of 30 min. On day 1, the escape platform was placed 1 cm above the water and was visible to the mice. During each trial, the mice facing the tank wall were released from three starting locations, except for the quadrant where the platform was in a random order, and the time spent to find the escape platform was recorded. If the mice failed to find the platform within 90 s, they were gently guided to the platform and allowed to remain there for 20 s; the escape time was recorded as 90 s. On day 2–5, the tests were performed as per the procedure on day 1, except that the platform was submerged 1 cm below the water surface. During the learning phase, the latency period of three points for each mouse to find the platform was recorded and the average value was calculated. In the testing phase, the platform was removed and the mice facing the pool wall were placed in the pool from the point furthest away from the platform. The mice were allowed to swim freely in the water maze for 90 s, after which they were returned to their cages. The number of times the mouse crossed the platform, the time spent in the target quadrant, and the swimming speed were recorded by a camera and analyzed using a behavior analyzing system (Topscanlite 3.0).

2.5. Immunostaining and imaging

90 min after FST or the last behavior test was performed, the mice were deeply anesthetized with 1% isoflurane and transcardially perfused with 30 mL of 0.9% NaCl, followed by 30 mL of 4% paraformaldehyde (PFA) (30525-89-4, Sigma, 0.01M PBS, pH 7.4). Then, the brain was quickly removed and fixed overnight in 4% PFA solution at 4 °C. Over the following two days, the brain was sequentially cryoprotected with 15% and 30% sucrose solutions at 4 °C (57-50-1, Sigma, 0.2 M PB, pH 7.4). After cryoprotection, the brain was cut into 30 μm coronal sections using a cryostat (Leica). The sections were rinsed in 0.01 M PBS (pH 7.4) five times for 6 min. Brain slices were put in 0.01 M PBS containing 5% bovine serum albumin (BSA, CAS9048-46-8, GENVIEW) and 1% Triton X-100 (CAS9002-93-1, BIOFROXX) at room temperature for 1 h. Then, the brain slices were placed into the primary antibody for incubation at 4 °C for 48 h. Primary antibody was prepared using a 0.01 M PBS solution, containing 1% BSA and 1% Triton X-100. Following that, the slices were rinsed in 0.01 M PBS for five times of 6 min and incubated with secondary antibody at 4 °C for 48 h. The primary antibodies used in the experiment were rabbit anti-c-Fos (1:300, CST2250s; Cell Signaling Technology), mouse anti-CaMKIIα (1:100, ab22609; Abcam), mouse anti-GAD67 (1:200, Mab5406; Millipore), and mouse anti-Orexin B (1:500, MAB734; R&D). The following secondary antibodies were used: AlexaFluor 555 anti-mouse IgG (1:1000, A31570; Invitrogen) and AlexaFluor 488 anti-rabbit IgG (1:1000, A21206; Invitrogen). Finally, the sections were mounted on gelatin-coated slides and covered with Fluoro-Gel containing DAPI (17985-50, Electron Microscopy Sciences). Fluorescent images were captured using a digital camera mounted on a DMI6000B microscope (Leica). All images were analyzed using ImageJ software. In each mouse, the number of neurons per unit area was calculated from four consecutive brain slices.

2.6. Immunohistochemistry

Sections were prepared for immunofluorescence analysis as described above. They were washed with PBS (0.01 M) three times for 10 min and then incubated in 0.3% H_2O_2 at room temperature for 30 min. After that, the sections were incubated at 4 °C with rabbit anti-c-Fos antibody (1:300 dilution, Rabbit CST2250s, Cell Signaling Technology) for 48 h. After rinsing, the sections were incubated with biotinylated anti-rabbit IgG (BA1000, Vector Laboratories) at room temperature for 2 h, washed with 0.01 M PBS five times for 6 min, and incubated in avidin-biotin complex (PK6100, Vector Laboratories, peroxidase) for 2 h at room temperature. Sections were rinsed, followed by 0.05% DAB (SK4100, Vector Laboratories) in 0.03% H_2O_2 for 5 min, washed five times for 6 min in PBS, mounted onto gelatin-coated slides, air-dried, dehydrated using graded ethanol, vitrified with dimethylbenzene, coverslipped with resins, and images were captured using a microscope (DM6000B, Leica). All images were analyzed using ImageJ

software. In each mouse, the number of c-Fos-labeled neurons per unit area was calculated from four consecutive brain slices.

2.7. Virus injection and optical fiber implantation

The surgical procedure has been previously described (Zheng et al., 2022). The mice were deeply anesthetized with 1% isoflurane and fixed on a brain stereotaxic equipment (68045, RWD). Erythromycin eye ointment was applied to the eyes of the mice to prevent corneal dryness and blindness, which may result from prolonged exposure to light. The surface hair of the skull was shaved, and the skin above the skull was carved. The skull surface was gently wiped with a cotton swab, the fontanelle was exposed, and a microsyringe was used to identify the origin of the fontanelle, followed by front, back, left, and right leveling. Then, we adjusted the microsyringe (LEGATO 130, RWD) to LH (ML: ±1.05 mm; AP: −1.25 mm; DV: −5.2 mm). A small hole (1 mm in diameter) was drilled into the skull surface, and the injection was performed at a rate of 50 nL/min.

For in vivo chemogenetic activation, AAV2/9-CaMKIIα-hM3Dq-EGFP (3×10^{12} GC/mL, PT-0525, BrainVTA) or AAV2/9-CaMKIIα-EGFP (3×10^{12} GC/mL, PT-0290, BrainVTA) was injected bilaterally into the LH at a volume of 0.2 μL for each site.

For in vivo chemogenetic inhibition, AAV2/9-CaMKIIα-hM4Di-mCherry (3×10^{12} GC/mL, PT-0524, BrainVTA) or AAV2/9-CaMKIIα-mCherry (3×10^{12} GC/mL, PT-0290, BrainVTA) were injected into the LH bilaterally at a volume of 0.2 μL for each site.

For optogenetic activation, AAV2/9-CaMKIIα-ChR2-EGFP (3×10^{12} GC/mL, S0166-9-H20, TaiTool) or AAV2/9-CaMKIIα-EGFP (3×10^{12} GC/mL, S0242-9-H20, TaiTool) was injected unilaterally into the LH at a volume of 0.2 μL.

For in vivo fiber photometry, AAV2/9-CaMKIIα-GCaMP6m (3×10^{13} GC/mL, S0481-9-H5, TaiTool) diluted with 0.01M PBS (1:3), AAV-vGAT-GCaMP6m (3×10^{12} GC/mL, PT-0346, BrainVTA) were injected unilaterally into the LH at a volume of 0.2 μL. After injection, the glass pipette was left in place for an additional 10 min and then slowly extracted to prevent virus leakage into the track.

For optogenetic activation and in vivo calcium signal recording, optical fibers (diameter: 200 μm, AG–FOC–W-1.25-200-0.37-6.0, Nanjing Aoguan Biotechnology Co.Ltd, Nanjing, China) with a ceramic ferrule were implanted into the LH (ML: ±1.05 mm; AP: −1.25 mm; DV: −5.2 mm) according to previous literature. Three miniature screws (1 mm diameter, 3 mm length) were fixed on the skull, and dental cement was used to connect the skull, screws, and optical fibers for structural support.

Finally, the wound was sutured and lincomycin hydrochloride gel (CYHS0800339, Shanghai New Asia Pharmaceutical Co. Ltd., China) was applied to the surface of the surgical wound, the gel should cover the wound completely. The mice were placed in a warm chamber and returned to their cages after recovery. Only the mice with verified injection sites were included in the analysis.

2.8. In vivo chemogenetic stimulation

For chemogenetic stimulation, 21 days after virus injection, the mice of all groups were intraperitoneally injected with Clozapine N-oxide (CNO) (3.3 mg/kg, C0832, Sigma) 45 min before each behavioral test.

2.9. In vivo optogenetic activation

For in vivo optogenetic activation, the optic fiber was assembled as described following the protocol (Jennings et al., 2013). Behavioral tests were performed 21 days after the virus injection. Blue light (465 nm, 40 Hz, 5 ms, 10 mW) was used to activate LH glutamatergic neurons via optical fiber connected with a laser source (B1-465, Inper LLC).

2.10. In vivo fiber photometry recording

In vivo fiber photometry was performed as previously described (Tang et al., 2022). Three weeks after SNI surgery, AAV-CaMKIIα-G-CaMP6m and AAV-vGAT-GCaMP6m was injected into the LH, and an optical fiber (diameter: 200 μm) with a ceramic ferrule were implanted 0.1 mm above the injection sites as described above. The mice were allowed to recover for 21 days before the experiments were performed. Fluorescence signals of the LH neurons were recorded during the FST using a fiber photometry system (FPS-410/470, Inper) that connected to the recording system to allow FST by rotating swivel. Mice were considered immobile when they were floating without any other movement. Time 0 was defined as the moment when subject animals began to mobile following a period of immobility. The fiber photometry system was equipped with 470 nm and 410 nm excitation lasers. Excitation fluorescence at 470 nm was used to measure neuronal activity and 410 nm was used as a control for motion and bleach pairs. Photometric data of control and SNI mice were subjected to autofluorescence background subtraction and imported into MATLAB for further analysis. (F–F0)/F0 was calculated as fluorescence change (ΔF/F) and heat maps are presented. Post hoc histology was performed to verify the accuracy of viral infection and optic fiber implantation. The data of the mice that deviated from the location were excluded from the analysis.

2.11. Quantification and statistical analysis

All data were analyzed using the Prism 9.2 statistical Software package (GraphPad Software). Normal distribution and similar variance within each comparison group were checked before parametric analyses. The paw withdrawal threshold PWT at multiple time points was measured with Von Frey test and compared by two-way analysis of variance (ANOVA) followed by Bonferroni's post hoc test. Comparison between the two groups, an unpaired student's t-test was used. Comparison of four groups, two-way ANOVA with Bonferroni's post hoc tests was used. The sample size chosen for each study was established by previous pilot and published studies. The post-hoc p values were presented where necessary in result section. All F (and degrees of freedom) and the p value of the time/group interaction have been displayed in Supplementary Table 1. Results were considered significantly different at $P < 0.05$. All data were calculated as Mean ± SEM.

3. Results

3.1. Chronic pain induced anxiety, depression, and learning and memory impairment

Previous studies have demonstrated that chronic pain induces mood disorders and learning and memory impairment (Narita et al., 2006; Wang et al., 2023; Yamauchi et al., 2022; Zhang et al., 2022). In the present study, the SNI was used to establish a mouse model of neuropathic pain (Supplementary Fig. 1A). The von Frey test was performed one day before the SNI operation (Fig. 1A). The results showed that the mechanical PW threshold did not differ between the sham and SNI groups before surgery. The PW threshold significantly decreased in the SNI group from 1 to 6 weeks after surgery, suggesting that SNI induces long-term neuropathic pain ($P < 0.001$. Fig. 1B).

Behavioral tests were performed at 2 (Supplementary Figs. 1B–C), 4 (Supplementary Figs. 1H–I), and 6 weeks (Fig. 1A and B) after the operation in different animals. First, we assessed the effect of chronic pain on anxiety-like behavior. Behavioral results showed that at 2 and 4 weeks after the operation, the two groups did not differ significantly in the open field test (OFT) (duration in center: 2W $P = 0.091$; 4W $P = 0.516$. moving distance: 2W $P = 0.408$; 4W $P = 0.068$. Supplementary Fig. 1D-E, and J-L), while mice in the SNI 6W group spent less time in the center area than the sham group, and there was no difference in moving distance (duration in center: $P = 0.043$; moving distance: $P = 0.666$.

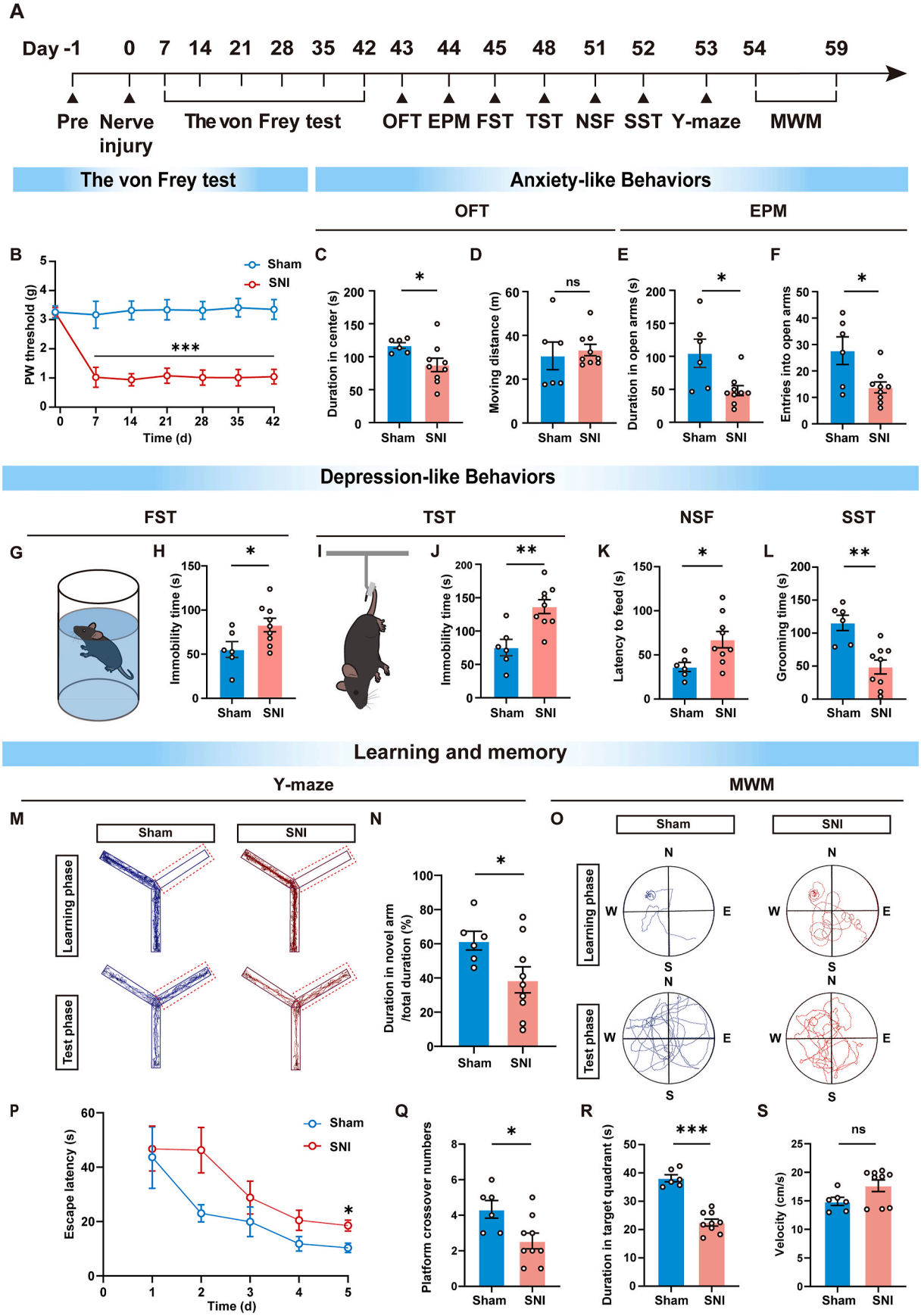

(caption on next page)

Fig. 1. Chronic pain induced anxiety, depression, and learning and memory impairment.
(A) Experimental schedule of the spared nerve injury (SNI) and behavioral tests. (B) Mechanical paw withdrawal (PW) threshold of sham mice and SNI mice (sham: n = 6; SNI: n = 9. Two-way repeated measures ANOVA with Bonferroni's post hoc test). (C–D) The open field test (OFT) was performed 6 weeks after SNI. (C) The SNI mice spent less time in the center (sham: n = 6; SNI: n = 9. Unpaired student's t-test). (D) There was no difference in moving distance (sham: n = 6; SNI: n = 9. Unpaired student's t-test). (E–F) The elevated plus maze (EPM) was performed 6 weeks after SNI. (E) The SNI mice spent less time in open arms (sham: n = 6; SNI: n = 9. Unpaired student's t-test). (F) The number of entering open arms in SNI mice was less (sham: n = 6; SNI: n = 9. Unpaired student's t-test). (G) Schematic diagram of forced swimming test (FST) in SNI and sham mice. (H) The immobility time in the FST (sham: n = 6; SNI: n = 9. Unpaired student's t-test). (I) Schematic diagram of tail suspension test (TST) in SNI and sham mice. (J) The immobility time in the TST (sham: n = 6; SNI: n = 9. Unpaired student's t-test). (K) The SNI mice spent more time in reaching food in the novelty suppression feeding test (NSF) (sham: n = 6; SNI: n = 9. Unpaired student's t-test). (L) The grooming time of SNI mice was less than that of sham mice in the sucrose splash test (SST) (sham: n = 6; SNI: n = 9. Unpaired student's t-test). (M) Representative animal traces of the Y maze in the sham and SNI mice. (N) The SNI mice spent less time in novel arm than the sham mice in the Y maze (sham: n = 6; SNI: n = 9. Unpaired student's t-test). (O–S) The Morris water maze (MWM) was performed 6 weeks after SNI. (O) Representative animal traces of the MWM (up panel represents learning traces on day 5, bottom panel represents test phase on day 6) in the sham and SNI mice. (P) Escape latency in locating the submerged platform of the mice in the learning phase (sham: n = 6; SNI: n = 9. Two-way repeated measures ANOVA with Bonferroni's post hoc test). (Q) The number of crossing platform in the SNI mice was less (sham: n = 6; SNI: n = 9. Unpaired student's t-test). (R) The SNI mice spent less time in target quadrant than the sham mice (sham: n = 6; SNI: n = 9. Unpaired student's t-test). (S) There was no difference in velocity of the SNI and sham mice, (sham: n = 6; SNI: n = 9. Unpaired student's t-test). Data were presented as the mean ± SEM. $^{*}P < 0.05$, $^{**}P < 0.01$, $^{***}P < 0.001$.

Fig. 1C and D). In EPM test, 6 weeks after the operation, mice in the SNI group exhibited a reduced exploration time in the open arms and a decreased number of entries into the open arms compared to the sham group mice (duration in the open arms: $P = 0.012$; number of entries into open arms: $P = 0.014$. Fig. 1E and F). These results indicate that long-term chronic pain induces anxiety-like behavior in mice.

Subsequently, depression-like behavior was detected. FST and TST witnessed no statistical differences between the sham and SNI groups at 2 and 4 weeks after the operation (FST: 2W $P = 0.889$; 4W $P = 0.117$. TST: 2W $P = 0.701$; 4W $P = 0.609$. Supplementary Fig. 1F-G, and M-N), while the immobility time of mice in the SNI 6W group was increased compared to that in the sham group (FST: $P = 0.036$; TST: $P = 0.002$. Fig. 1G–J). Additionally, in NSF test, the latency to bite a food pellet was higher in SNI 6W mice than in the sham group ($P = 0.025$. Fig. 1K). In the SST mice in the SNI group spent less time grooming than those in the sham group ($P = 0.001$. Fig. 1L). Thus, we confirmed that chronic pain induces depression-like behavior in mice.

Furthermore, we used the Y maze and MWM to test the learning and memory abilities of the mice six weeks after surgery. In the Y-maze test, the percentage of duration in the novel arm reflected the spatial memory of the mice (Fig. 1M). Compared with the sham group, mice in the SNI group entered the novel arm less frequently, suggesting that chronic pain impaired memory function in mice ($P = 0.046$. Fig. 1N). The first day of the learning phase of the MWM witnessed no significant differences between the latency times of the sham and SNI groups to reach the platform, but the SNI group needed more time to reach the platform on the fifth day, indicating that chronic pain decreased their learning ability ($P = 0.026$. Latency of fifth day: $P = 0.041$. Fig. 1O-P). After the learning phase, the platform was removed from the pool for a 90 s probe trial. The results showed that the duration in the target quadrant and the number of target crossing for the SNI group mice were significantly decreased compared with these of sham group (number of target crossing: $P = 0.021$; duration in the target quadrant: $P < 0.001$. Fig. 1Q-R). We further analyzed the experimental results for the velocity in the MWM ($P = 0.069$. Fig. 1S), indicating that SNI did not significantly impair the motor function in mice. In summary, chronic pain induces learning and memory impairment.

Therefore, mice with chronic pain may exhibit anxiety- and depression-like behaviors and learning and memory impairment.

3.2. *Glutamatergic neuronal activity increased in lateral hypothalamus of chronic pain mice*

The above results indicate that chronic pain induces significant anxiety- and depression-like behaviors and impairs learning and memory. Several studies have shown that the hypothalamus plays an important role in maintaining the stability of animal behavior. The hypothalamus has a complex anatomical structure. Accordingly, the following nuclei in the hypothalamus that are closely related to mood disorders were selected for our study: MPO, PVN, AHN, LH, VMH, DMH, Arc, and SUM. To clarify which region of the hypothalamus was mainly involved in chronic pain-induced behavioral dysfunction, the brain slices of the sham and SNI mice were labeled with c-Fos after the FST (Fig. 2A, Supplementary Figs. 2A–G). We found that the expression of c-Fos in the MPO, VMH, DMH, Arc, SUM, and AHN were not significantly different between mice in the SNI and sham groups, but in the PVN and LH, they were increased in SNI mice, whereas c-Fos expressions in the LH were the most obvious (MPO: $P = 0.122$; PVN: $P = 0.023$; DMH: $P = 0.797$; VMH: $P = 0.997$; LH: $P = 0.021$; Arc: $P = 0.279$; SUM: $P = 0.264$; AHN: $P = 0.549$. Fig. 2B).

It is known that LH mainly consists of excitatory cells that can be immunolabeled by CaMKIIα antibody (CaMKIIα+) and inhibitory GABAergic interneurons that can be immunolabeled by GAD67 antibody (GAD67+). Besides, neurons expressing hypocretin/orexin (Hcrt/Ox) that can be immunolabeled by OXB antibody (OXB+) appear to be uniquely found within the LH. To determine which type of neurons in the LH were involved in anxiety- and depression-like behaviors and learning and memory dysfunction after chronic pain, the co-localization of c-Fos with CaMKIIα, GAD67 and OXB was analyzed on brain slices of SNI mice and control mice. In the LH of control mice, a small number of c-Fos+ and CaMKIIα+, GAD67+ or OXB + co-labeled neurons were found. After SNI treatment, the density of CaMKIIα+ and c-Fos + co-labeled cells increased significantly, but the density of GAD67+ or OXB+ and c-Fos + co-labeled cells remained still (c-Fos+ and CaMKIIα+: $P = 0.006$; c-Fos+ and GAD67+: $P = 0.601$; c-Fos+ and OXB+: $P = 0.725$. Fig. 2C and D, Supplementary Figs. 3A–D). These results indicate that CaMKIIα expressing neurons in the LH were selectively hyperactivated in SNI mice during FST behavior test but not in normal mice.

We utilized fiber photometry in vivo to assess whether LH neuronal activity is associated with emotion under chronic pain condition. AAV2/9- CaMKIIα-GCaMP6m or AAV2/9-vGAT-GCaMP6m were delivered into LH by stereotaxic injection to express the Ca^{2+} indicator GCaMP6m in LH glutamatergic neurons or GABAergic neurons, and an optical fiber was implanted into the injection site (Fig. 2E–H, and Supplementary Figs. 3E–G). Dynamic calcium signals during the FST were recorded using in vivo fiber photometry. The calcium signal activity of glutamatergic neurons in the SNI group was significantly higher than that in the sham group when the mice began to mobile ($P < 0.001$. Fig. 2I–K). However, the calcium signals of GABAergic neurons did not differ between SNI and sham mice ($P = 0.524$. Supplementary Figs. 3H–J). These results suggest that the alteration in immobility time during the FST is related to the enhanced response of LH glutamatergic neurons in SNI mice.

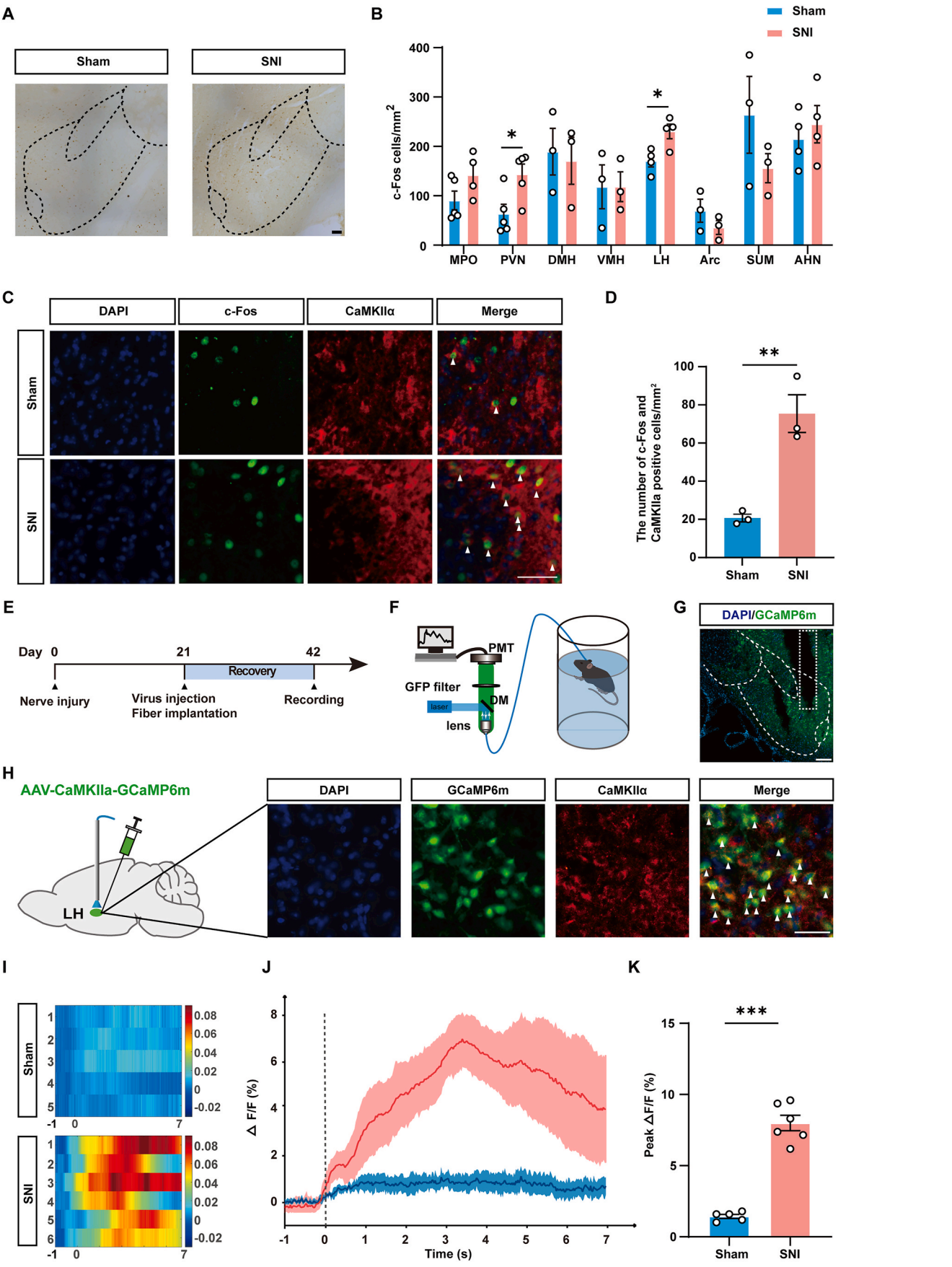

(caption on next page)

Fig. 2. The glutamatergic neurons in the lateral hypothalamus (LH) of SNI mice were activated after FST exposure.
(A) The c-Fos positive cells of the sham and SNI mice in LH 90 min after FST. (B) The mean density of c-Fos positive cells in the MPO (sham: n = 5; SNI: n = 4. Unpaired student's t-test); PVN (sham: n = 5; SNI: n = 5. Unpaired student's t-test); DMH (sham: n = 3; SNI: n = 3. Unpaired student's t-test); VMH (sham: n = 3; SNI: n = 3. Unpaired student's t-test); LH (sham: n = 4; SNI: n = 4. Unpaired student's t-test); Arc (sham: n = 3; SNI: n = 3. Unpaired student's t-test); SUM (sham: n = 3; SNI: n = 3. Unpaired student's t-test); AHN (sham: n = 4; SNI: n = 4. Unpaired student's t-test). (C) Merged confocal image of DAPI (Blue), c-Fos (Green) co-stained with CaMKIIα (Red) in LH slices. The white arrowheads indicate the colocalized cells that expressed both c-Fos and CaMKIIα neurons. Scale bar, 50 μm. (D) The density of c-Fos and CaMKIIα co-labeled cells were measured (sham: n = 3; SNI: n = 3. Unpaired student's t-test). (E) Experimental schedule for recording dynamic Ca^{2+} signals of LH glutamatergic neurons. (F) Schematic diagram of recording dynamic Ca^{2+} signals of LH during FST. (G) Schematic diagram of injecting AAV-CaMKIIα-GCaMP6m virus into LH of the sham and SNI mice. Scale bar, 100 μm. (H) Double-staining of GCaMP6m (Green) and CaMKIIα (Red) and the corresponding merge images in LH of AAV2/9-CaMKIIα-GCaMP6m injection mice. The white arrowheads indicate the colocalized cells in the GCaMP6m and CaMKIIα neurons. Scale bar, 100 μm. (I) Heatmap showing Ca^{2+} signals of LH glutamatergic neurons aligned to the onset of mobile in the FST. Each row represents a trial. (J) Representative line of the averaged Ca^{2+} signals of LH glutamatergic neurons. (K) Summary plots of the ΔF/F signal of LH glutamatergic neurons (sham: 5 trails from 3 mice; SNI: 6 trails from 6 mice. Unpaired student's t-test). Data were presented as the mean ± SEM. $^{*}P < 0.05$, $^{**}P < 0.01$, $^{***}P < 0.001$. (For interpretation of the references to color in this figure legend, the reader is referred to the Web version of this article.)

3.3. Chemogenetic activation of LH glutamatergic neurons induced depression-like behaviors and learning and memory impairment in mice

To confirm the role of LH glutamatergic neurons activation in anxiety- and depression-like behaviors and cognitive dysfunction, we used chemogenetic techniques to selectively activate these neurons. AAV-CaMKIIα-EGFP or AAV-CaMKIIα-hM3Dq-EGFP was delivered into LH bilaterally in normal mice (Fig. 3A and B). The virus was abundantly expressed in CaMKIIα+ neurons in the LH after 21 days (Fig. 3C and D). Immunofluorescent staining showed that the intraperitoneal injection of CNO 45 min before the test selectively increased c-Fos expression in the LH ($P = 0.006$. Fig. 3E and F).

First, we examined the effect of the activation of LH glutamatergic neurons on mechanical stimuli using the von Frey test. The results showed no differences in the PW threshold for mechanical stimuli between the EGFP and hM3Dq groups ($P = 0.071$. Fig. 3G).

Next, we examined the effect of active LH glutamatergic neurons on anxiety-like behavior. In the OFT, hM3Dq-injection did not affect the duration in the center or the total moving distance (duration in the center: $P = 0.120$; moving distance: $P = 0.167$. Fig. 3H and I). Similarly, hM3Dq-injected mice did not change the duration or number of entries into the open arms in the EPM test compared to EGFP-injected mice (duration in open arms: $P = 0.935$; number of entries into open arms: $P = 0.408$) (Fig. 3J and K). Thus, activation of LH glutamatergic neurons did not induce anxiety-like behaviors in normal mice.

Third, depression-like behavior was detected after the activation of LH glutamatergic neurons. The results showed that the hM3Dq-injection did not change the immobility time in the FST or TST (FST: $P = 0.166$; TST: $P = 0.058$. Fig. 3L-M). The activation of LH glutamatergic neurons increased the latency to bit food pellets in the NSF test, and no significant differences were observed in the latency to feed in the home cage (latency to feed in an unfamiliar environment: $P = 0.018$; latency to feed in the home cage: $P = 0.377$. Fig. 3N-O). hM3Dq-injection decreased grooming time in the SST ($P = 0.030$. Fig. 3P). These results suggest that the activation of LH glutamatergic neurons recapitulates some of the depression-like behavior in normal mice.

In the Y maze, hM3Dq-injection significantly decreased the duration in the novel arm in normal mice ($P < 0.001$. Fig. 3Q). However, in the MWM, hM3Dq-injection had no significant influence on escape latency during the learning period ($P = 0.231$. Fig. 3R) but decreased platform crossover numbers and duration in the target quadrant during the testing period (number of crossings of the platform: $P = 0.020$; duration in the target quadrant: $P = 0.005$. Fig. 3S-T). These results suggest that the activation of LH glutamatergic neurons significantly impairs the learning and memory in normal mice.

3.4. Optogenetic activation of LH glutamatergic neurons induced depression-like behaviors and learning and memory impairment

To further clarify the relationship between the overactivation of LH glutamatergic neurons and behavioral abnormalities, optogenetic activation was used to control the activation of LH glutamatergic neurons on a millisecond scale during behavioral tests (Fig. 4A). AAV-CaMKIIα-EGFP or AAV-CaMKIIα-ChR2-EGFP were injected into the LH of normal mice, and optical fiber was implanted into the LH (Fig. 4B). The virus was abundantly expressed in CaMKIIα+ neurons in the LH after 21 days (Fig. 4C and D). The highest firing frequency of LH excitatory neurons has been reported as 40 Hz (Zheng et al., 2022). To ensure the effectiveness of the virus, brain slices were immunolabeled with c-Fos, and more c-Fos^{+} cells were observed in the LH of ChR2-injected mice than in EGFP-injected mice after blue light (10 mW, 40 Hz, 5 ms) was delivered into the LH ($P = 0.001$. Fig. 4E and F). In the von Frey test, optogenetic activation of LH glutamatergic neurons did not alter mechanical allodynia ($P = 0.308$. Fig. 4G).

The OFT witnessed no statistical differences between the two groups in the duration in the center area of the open field and the total moving distance in the open field (duration in the center: $P = 0.807$; moving distance: $P = 0.873$. Fig. 4H and I). In the EPM, optogenetic activation of LH glutamatergic neurons did not significantly change the number of entering open arms or the duration of exploration in the open arms (number of entering open arms: $P = 0.499$; duration in open arms: $P = 0.667$. Fig. 4J and K). Thus, consistent with the results of chemogenetic activation, the optogenetic activation of LH glutamatergic neurons did not induce anxiety-like behavior in normal mice.

In the FST and TST, there were no statistically significant differences in the immobility time between the ChR2-injection and EGFP-injection groups (FST: $P = 0.283$; TST: $P = 0.943$. Fig. 4L-M). However, in the NSF test, the latency to bit food for mice injected with ChR2 was significantly longer than that for mice injected with EGFP after blue light stimulation. However, there was no difference in the latency of feeding in the home cage (latency of feeding in an unfamiliar environment: $P = 0.032$; latency of feeding in the home cage: $P = 0.588$. Fig. 4N-O). Optogenetic activation of LH during the SST experiment significantly reduced the total grooming time in mice injected with ChR2 compared to those injected with EGFP ($P = 0.020$. Fig. 4P). Specific activation of glutamatergic neurons in the LH could induce depression-like behavior in normal mice.

In the Y maze, the exploration duration in the novel arm in the ChR2 group was significantly shorter than that in the EGFP group ($P = 0.006$. Fig. 4Q). In the MWM, during the first four days of the learning phase, the escape latency was not different between the ChR2 and EGFP groups, but the escape latency of mice in the ChR2 group was significantly longer than that of the EGFP group on the fifth day ($P = 0.026$. Latency of fifth day: $P = 0.025$. Fig. 4R). Additionally, the number of platform crossings and duration of exploring the target quadrant significantly decreased in the ChR2 group (number of platform crossings: $P = 0.003$; duration in the target quadrant: $P = 0.019$. Fig. 4S-T). Thus, these results further prove that the activation of glutamatergic neurons in the LH induces learning and memory impairment in normal mice.

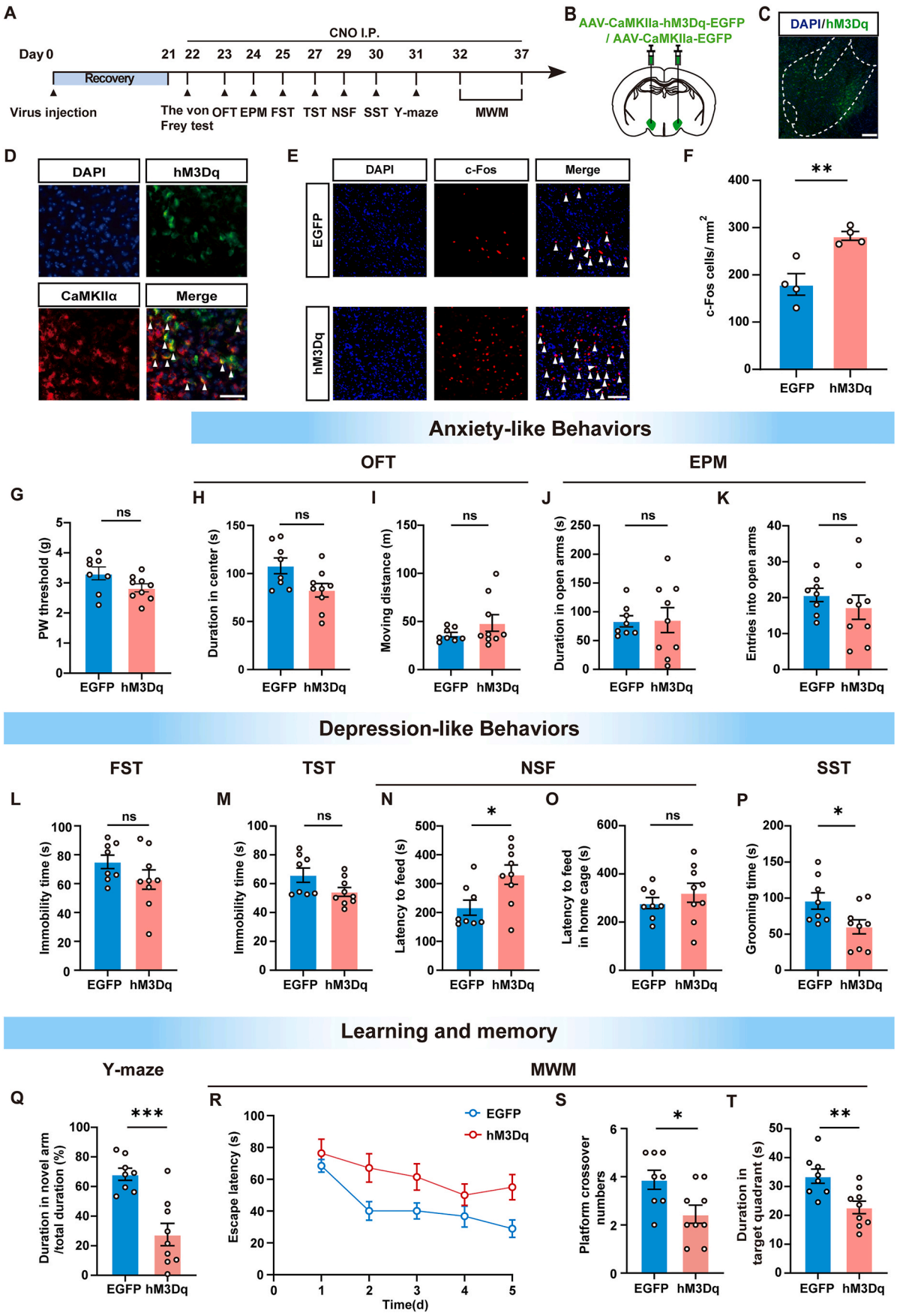

(caption on next page)

Fig. 3. Chemogenetic activation of LH glutamatergic neurons induced depression-like behaviors and learning and memory impairment in normal mice.
(A) Experimental schedule of virus injection and behavioral tests. (B) Schematic of the coronal section of the mouse brain showed hM3Dq virus injection. (C) AAV-CaMKIIα-GCaMP6m virus expressed in LH. Bar = 100 μm. (D) Merged confocal image of DAPI (Blue), EGFP (Green) co-stained with CaMKIIα (Red) in LH slices. The white arrowheads indicate the colocalized cells that expressed both EGFP and CaMKIIα neurons. Scale bar, 100 μm. (E–F) The expression of c-Fos in LH increased after injection of CNO. Scale bar, 100 μm. (EGFP: n = 4; hM3Dq: n = 4. Unpaired student's t-test). (G) Mechanical PW threshold in the von Frey test (EGFP: n = 8; hM3Dq: n = 9. Unpaired student's t-test). (H–I) The OFT was performed after injection of CNO in EGFP and hM3Dq mice. (H) There was no difference in time spent in center (EGFP: n = 8; hM3Dq: n = 9. Unpaired student's t-test). (I) There was no difference in moving distance (EGFP: n = 8; hM3Dq: n = 9. Unpaired student's t-test). (J–K) EPM was performed after injection of CNO in EGFP and hM3Dq mice. (J) Duration in the open arms (EGFP: n = 8; hM3Dq: n = 9. Welch's *t*-test). (K) The number of entering into open arms (EGFP: n = 8; hM3Dq: n = 9. Unpaired student's t-test). (L) The immobility time in the FST (EGFP: n = 8; hM3Dq: n = 9. Unpaired student's t-test). (M) The immobility time in the TST (EGFP: n = 8; hM3Dq: n = 9. Unpaired student's t-test). (N–O) The NSF was performed after injection of CNO in EGFP and hM3Dq mice. (N) The latency for mice to feed in an unfamiliar environment (EGFP: n = 8; hM3Dq: n = 9. Unpaired student's t-test). (O) The latency for mice to feed in the home cage (EGFP: n = 8; hM3Dq: n = 9. Unpaired student's t-test). (P) The grooming time in the SST ($t_{(15)} = 2.389$. Unpaired student's t-test). (Q). Mice injected with hM3Dq virus spent less time in exploring the novel arm in Y maze (EGFP: n = 8; hM3Dq: n = 9. Unpaired student's t-test). (R–T) The MWM was performed after injection of CNO in EGFP and hM3Dq mice. (R) There was no difference in escape latency between the two groups (EGFP: n = 8; hM3Dq: n = 9. Two-way repeated measures ANOVA with Bonferroni's post hoc test). (S) Platform crossover numbers (EGFP: n = 8; hM3Dq: n = 9. Unpaired student's t-test). (T) Duration in target quadrant (EGFP: n = 8; hM3Dq: n = 9. Unpaired student's t-test). Data were presented as the mean ± SEM. $^{*}P < 0.05$, $^{**}P < 0.01$, $^{***}P < 0.001$. (For interpretation of the references to color in this figure legend, the reader is referred to the Web version of this article.)

3.5. Inhibition of LH glutamatergic neurons could alleviate anxiety- and depression-like behaviors and learning and memory impairment induced by chronic pain

The above experimental results suggest that the activity of LH glutamatergic neurons in SNI-treated mice increases after pain stimulation, and artificial activation of LH induces depression-like behaviors and learning and memory impairment. Therefore, we aimed to clarify whether inhibiting the activity of LH glutamatergic neurons in SNI mice could alleviate anxiety- and depression-like behaviors and learning and memory impairment induced by chronic pain. We used a chemogenetic inhibition technique to inhibit glutamatergic neurons in the LH of mice. AAV-CaMKIIα-hM4Di-mCherry or AAV-CaMKIIα-mCherry were injected into the LH bilaterally (Fig. 5A and B). hM4Di or mCherry was robustly expressed in the CaMKIIα+ neurons in the LH after 21 days (Fig. 5C and D) and CNO (3.3 mg/kg) was injected intraperitoneally 45 min before each behavioral test. Immunofluorescent staining showed that LH glutamatergic neurons in the mice injected into AAV-CaMKIIα-hM4Di-mCherry were specifically inhibited after CNO injection ($P = 0.003$. Fig. 5E and F).

Mice with SNI had a decreased PW threshold for mechanical stimuli, but hM4Di injection did not change the threshold for mechanical stimuli (sham-mCherry vs. sham-hM4Di, $P = 0.390$; sham-mCherry vs. SNI-mCherry, $P < 0.001$; SNI-mCherry vs. SNI-hM4Di, $P = 0.862$. Fig. 5G).

The OFT and EPM were used to examine the effects of inhibiting LH glutamatergic neurons on anxiety-like behavior. In the OFT, sham-hM4Di group mice showed similar duration in the center area compared to sham-mCherry group mice ($P > 0.999$. Fig. 5H). SNI-mCherry group mice showed a decreased duration in the center area compared to sham-mCherry group mice ($P = 0.024$. Fig. 5H). Compared to mCherry-expressing SNI mice, hM4Di-expression did not affect the duration spent in the center area ($P > 0.999$. Fig. 5H). In the EPM test, compared to mCherry-expressing sham mice, hM4Di-expression did not affect the duration and number of entering into the open arms (duration in open arms: $P = 0.670$. Number of entering into open arms: $P > 0.999$, Fig. 5I and J); compared with the sham-mCherry group, the duration and number of entering into the open arms significantly decreased in the SNI-mCherry group (duration in open arms: $P = 0.024$. Number of entering into open arms: $P = 0.026$. Fig. 5I and J). The duration and number of entering into open arms were increased in the SNI-hM4Di group compared with those in the SNI-mCherry group (duration in open arms: $P = 0.002$. Number of entries into open arms: $P = 0.005$. Fig. 5I and J). These results demonstrated that the inhibition of glutamatergic neurons in the LH of SNI mice partially alleviated anxiety-like behavior.

We tested whether the inhibition of LH glutamatergic neurons in SNI mice could relieve depression-like behavior induced by chronic pain. In the FST, there was no statistically significant difference in the immobility time between the in the sham-mCherry and sham-hM4Di group ($P > 0.999$. Fig. 5K); the immobility time in the SNI-mCherry group was higher than that in the sham-mCherry group ($P < 0.001$. Fig. 5K). Compared to the SNI-mCherry group mice, hM4Di-injection significantly decreased the elevated immobility time induced by chronic pain ($P < 0.001$. Fig. 5K). In the TST, there was no statistically significant difference in the immobility time between the in the sham-mCherry and sham-hM4Di group ($P = 0.817$. Supplementary Fig. 4A); SNI-mCherry group mice showed increased immobility time compared to sham-mCherry group mice ($P = 0.010$. Supplementary Fig. 4A). Accordingly, hM4Di-injection significantly decreased the duration of immobility induced by chronic pain ($P < 0.001$. Supplementary Fig. 4A). In the NSF, in an unfamiliar environment, mice in the sham-hM4Di group showed similar latency of feeding to the sham-mCherry group ($P = 0.340$. Fig. 5L); the latency of feeding in the SNI-mCherry group was significantly higher than that in the sham-mCherry group in an unfamiliar environment ($P = 0.011$. Fig. 5L). However, the latency of food biting was significantly lower in the SNI-hM4Di group than in the SNI-mCherry group ($P = 0.015$. Fig. 5L). There was no difference in the latency to find food in the home cages ($P > 0.999$, Supplementary Fig. 4B). In the SST, after spraying with 10% sucrose solution there was no statistically significant difference in the total grooming time between the in the sham-mCherry and sham-hM4Di group ($P > 0.999$. Fig. 5M); the total grooming time decreased in the SNI-mCherry group compared with that in the sham-mCherry group. Accordingly, grooming time was increased in the SNI-hM4Di group (sham-mCherry vs. SNI-mCherry, $P < 0.001$; SNI-mCherry vs. SNI-hM4Di, $P < 0.001$. Fig. 5M). These results suggest that inhibition of LH glutamatergic neuronal activity in SNI mice relieved depression-like behavior induced by chronic pain.

The Y maze results showed that there was no statistically significant difference in the duration in the novel arm between the in the sham-mCherry and sham-hM4Di group; mCherry-injected SNI mice spent less time in the novel arm than sham mice, but hM4Di-expression significantly prolonged the time spent in the novel arm compared with mCherry-expressing SNI mice (sham-mCherry vs. sham-hM4Di, $P = 0.721$; sham-mCherry vs. SNI-mCherry, $P = 0.029$; SNI-mCherry vs. SNI-hM4Di, $P = 0.032$. Fig. 5N). The MWM test witnessed no differences in escape latency during the learning phase ($P = 0.094$. Fig. 5O). In the testing phase, all mice displayed similar number of crossing the platform ($P = 0.174$. Supplementary Fig. 4C). Normal mice treated with hM4Di displayed similar duration in the target quadrant with the normal mice treated with mCherry ($P > 0.999$. Fig. 5P); duration in the target quadrant in the SNI-mCherry group decreased compared to the sham-mCherry group ($P = 0.021$. Fig. 5P). Accordingly, hM4Di-expression increased the number of crossing the platform and duration in the target quadrant ($P = 0.001$. Fig. 5P). These results indicate that the inhibition of glutamatergic neurons in the LH of SNI mice could relieve learning and memory impairment induced by chronic pain.

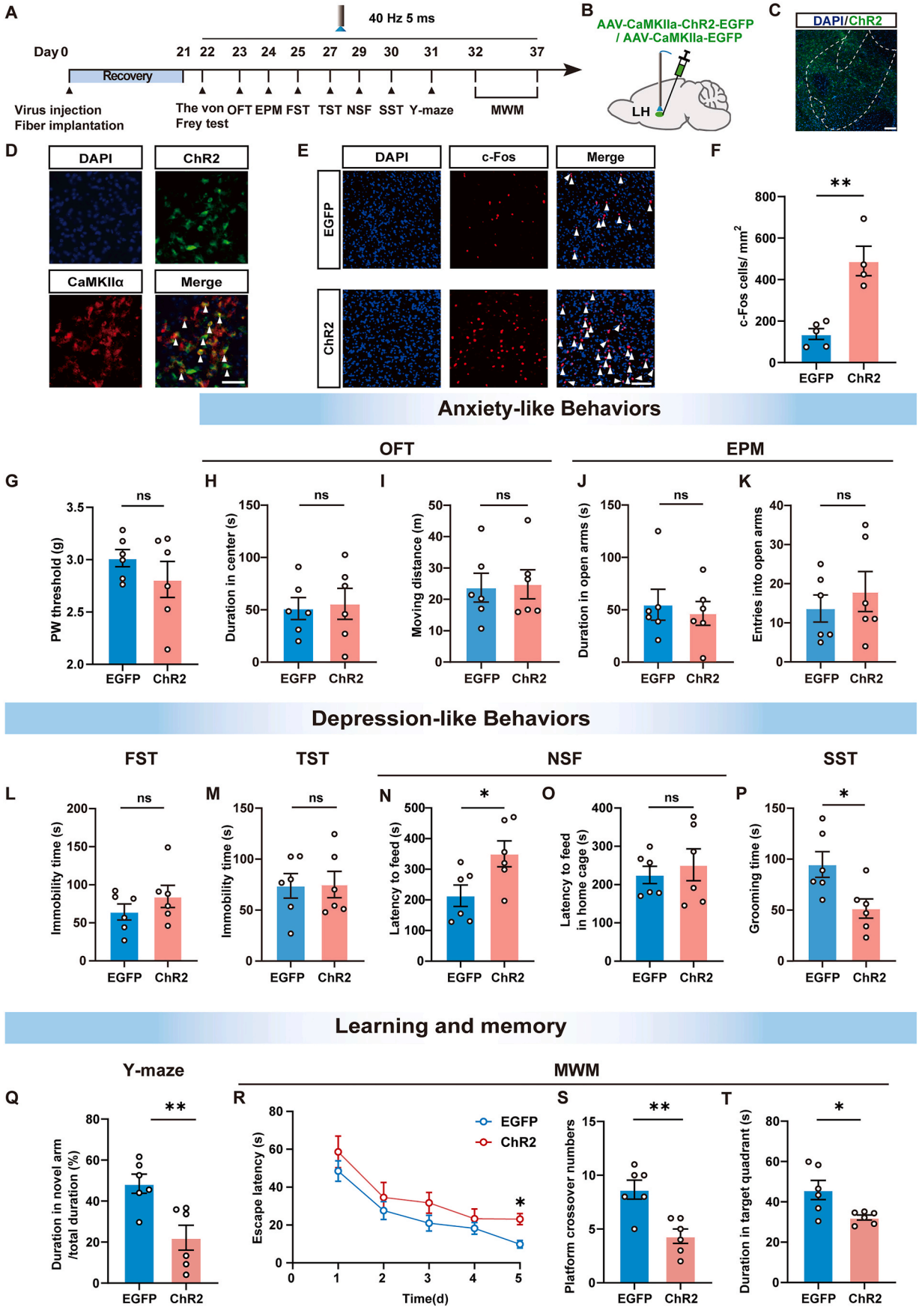

(caption on next page)

Fig. 4. Optogenetic activation of LH glutamatergic neurons induced depression-like behaviors and learning and memory impairment.
(A) Experimental schedule of virus injection and behavioral tests, blue light pulses at 40 Hz, 5 ms,10 mw. (B–C) Schematic of the coronal section of the mice brain showed ChR2 virus injection, bar = 100 μm. (D) Merged confocal image of DAPI (Blue), ChR2 (Green) co-stained with CaMKIIα (Red) in LH slices. The white arrowheads indicate the colocalized cells that expressed both ChR2 and CaMKIIα neurons. Scale bar, 100 μm. (E–F) The expression of c-Fos in LH increased in the mice injected with ChR2 virus after blue light delivery. Scale bar, 100 μm. (EGFP: n = 5; ChR2: n = 4. Unpaired student's t-test). (G) Mechanical PW threshold in the von Frey test (EGFP: n = 6; ChR2: n = 6. Unpaired student's t-test); (H–I) OFT was performed. (H) There was no difference in duration in center (EGFP: n = 6; ChR2: n = 6. Unpaired student's t-test). (I) There was no difference in moving distance (EGFP: n = 6; ChR2: n = 6. Unpaired student's t-test). (J–K) EPM was performed. (J) Duration in the open arms (EGFP: n = 6; ChR2: n = 6. Unpaired student's t-test). (K) The number of entering open arms (EGFP: n = 6; ChR2: n = 6. Unpaired student's t-test). (L) The immobility time in the FST (EGFP: n = 6; ChR2: n = 6. Unpaired student's t-test). (M) The immobility time in the TST (EGFP: n = 6; ChR2: n = 6. Unpaired student's t-test). (N–O) NST was performed. (N) The latency for mice to feed in an unfamiliar environment (EGFP: n = 6; ChR2: n = 6. Unpaired student's t-test). (O) The latency for mice to feed in the home cage (EGFP: n = 6; ChR2: n = 6. Unpaired student's t-test). (P) The grooming time in the SST (EGFP: n = 6; ChR2: n = 6. Unpaired student's t-test). (Q) Mice injected with ChR2 virus spent less time in exploring the novel arm in Y maze (EGFP: n = 6; ChR2: n = 6. Unpaired student's t-test). (R–T) MWM was performed. (R) Escape latency in locating the platform of the mice in learning phase (EGFP: n = 6; ChR2: n = 6. Two-way repeated measures ANOVA with Bonferroni's post hoc test). (S) Platform crossover numbers (EGFP: n = 6; ChR2: n = 6. Unpaired student's t-test). (T) Time in target quadrant (EGFP: n = 6; ChR2: n = 6. Unpaired student's t-test). Data were presented as the mean ± SEM. $^{*}P < 0.05$, $^{**}P < 0.01$. (For interpretation of the references to color in this figure legend, the reader is referred to the Web version of this article.)

4. Discussion

The neural mechanisms underlying mood disorders and learning and memory impairment induced by chronic pain remain unclear. We provided novel evidence indicating SNI-induced anxiety- and depression-like behaviors and learning and memory impairment in male mice, accompanied by overactivation of LH glutamatergic neurons. Investigating further, we manipulated these neurons using optogenetic and chemogenetic method, noting that their activation in normal mice triggered some of the depression-like behavior and learning and memory impairment without affecting anxiety-like behavior. Conversely, inhibiting these neurons in SNI mice effectively alleviated anxiety- and depression-like behaviors as well as learning and memory impairment. Thus, our results indicate that overactivation of LH glutamatergic neurons is involved in depression-like behavior and learning and memory impairment induced by SNI (see Fig. 6).

Chronic pain significantly correlates with higher risks of post-traumatic stress disorder (PTSD), major depressive disorder, anxiety disorder and alcohol use disorder (Morasco et al., 2013). Different models have been developed in rodents to study emotional changes after chronic pain, but have showed conflicting results about the association between chronic neuropathic pain and mood disorders, which may be caused by differences in the models of neuropathy employed, types and modalities of behavioral readouts, and time points of analysis post-injury (Kremer et al., 2021). In this study, behavioral changes in SNI mice were systematically tested at 2, 4, and 6 weeks after modeling, which demonstrated that SNI mice develop anxiety- and depression-like behaviors and learning and memory impairment by six weeks post-modeling. Many large-scale observational studies have indicated that chronic pain often coincides with the development of major depressive and anxiety disorders. Among the complicated etiologies of depression, chronic pain is a major risk factor (Kroenke et al., 2013; Rayner et al., 2016). Preclinical studies have reported depression- and anxiety-like behaviors in animal models of chronic pain, consistent with our results (Yamauchi et al., 2022; Zhou et al., 2019). Additionally, our results indicated that SNI mice exhibit significant cognitive decline in the Y maze and MWM tests, aligning with broader research linking chronic pain to cognitive impairments (Li et al., 2020; Zhang et al., 2022). This study reinforces the connection between chronic pain and anxiety- and depression-like behaviors and learning and memory impairment after six weeks of pain induction.

Brain imaging studies in humans and rodents have demonstrated that as pain becomes chronic, there is a progressive shift from nociceptive to emotionally governed networks (Davis et al., 2017). There is a robust decline in volume following pain induction in several brain regions that form part of the nociceptive network as well as the limbic system (Davis and Moayedi, 2013; Mayer et al., 2015). Animal studies have shown that chronic pain causes structural remodeling in brain structures, including the medial prefrontal cortex (mPFC), such as a reduction in length and arborization of proximal apical dendrites, which alters the function of glutamate receptors and results in cognitive impairment (Kelly et al., 2016). The hypothalamus is a part of the limbic system and plays an important role in reward, motivation, and learning and memory (Burdakov and Peleg-Raibstein, 2020; Ferrario and Finnell, 2023; Hu et al., 2021; Otis et al., 2019). We found that the activities of the MPO, VMH, DMH, Arc, SUM, and AHN did not change significantly, whereas LH glutamatergic neurons were selectively activated after exposure to SNI. The LH is extensively interconnected with multiple brain regions such as the mPFC, lateral septum (LS), and nucleus accumbens (NAc) (Chen et al., 2022). LH is involved in regulating arousal, feeding, energy balance, stress, rewards, and motivational behaviors (Bonnavion et al., 2016). The LS GABAergic projection to the LH plays an important role in regulating anxiety comorbidities (Wang et al., 2023). Inhibition of LH neuron terminals in the ventral tegmental area (VTA) facilitates the learning of reward-paired cues in mice (Sharpe et al., 2017). Our results are consistent with those in the literature, and indicate that LH may plays an important role in anxiety- and depression-like behaviors and learning and memory.

There are two types of neurons in the LH: glutamatergic and GABAergic. We found that glutamatergic neuronal activity in the LH increased after chronic pain. Numerous studies have shown that glutamatergic neurons in the LH play important functional roles in reward and motivational behaviors, motivational behaviors (Floresco, 2015; Hashmi et al., 2013; Lazaridis et al., 2019; Schwartz et al., 2014; Zinsmaier et al., 2022). Our results and recent research further confirmed that direct activation of glutamatergic neurons in the LH impaired learning and memory in mice (Lazaridis et al., 2019). Accordingly, the inhibition of LH glutamatergic neurons in SNI mice could alleviate learning and memory impairment. In addition, several studies have shown that LH glutamatergic neurons play an important role in the regulation of mood-related disorders. In rodents, the FST, TST, NSF and SST are commonly used to detect the depression-like behavior (Dai et al., 2022; Hao et al., 2019; Willner et al., 1987). In response to stress, the LH exhibits a unique firing pattern that drives LHb excitatory post-synaptic potential (EPSP) to reliably induces symptoms of depression (Zheng et al., 2022). Therefore, in our study, the activation of LH glutamatergic neurons in normal mice induced depression-like behavior. Accordingly, the chemogenetic inhibition of LH glutamatergic neurons in SNI mice effectively alleviated behavioral abnormalities.

However, chemogenetic and optogenetic activation of glutamatergic neurons in the LH of normal mice did not result in anxiety-like behavior, but chemogenetic inhibition of glutamatergic neurons in the LH significantly rescued SNI-induced anxiety-like behavior. We hypothesize that this discrepancy may due to the fact that glutamatergic neurons within the lateral hypothalamus (LH) can be divided into two subpopulations. These two subpopulations may respectively attenuate and promotes anxiety-like behavior when activated. In normal mice, both groups of neurons are at a lower baseline level of excitation, so chemogenetic or

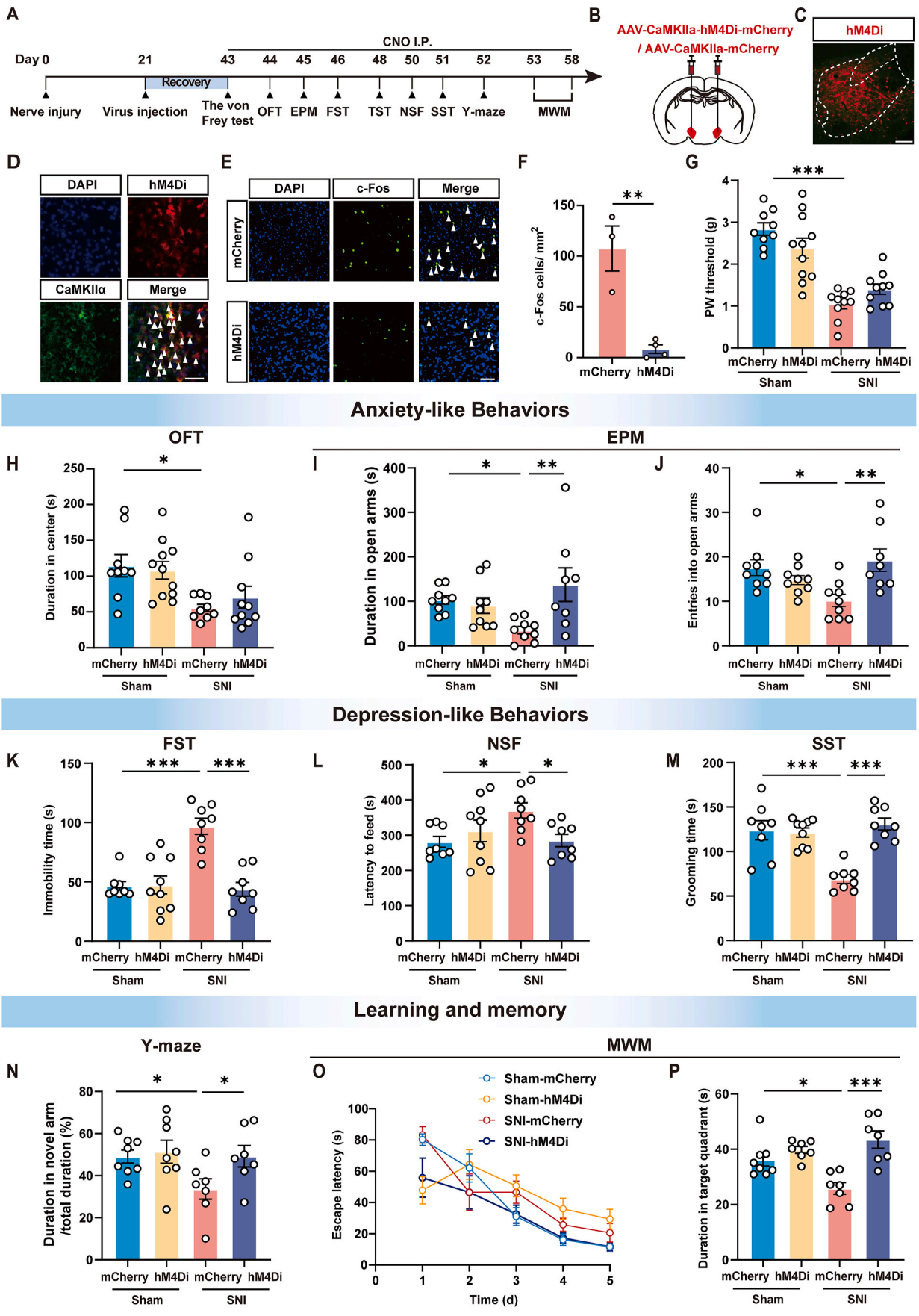

(caption on next page)

Fig. 5. Inhibition of LH glutamatergic neurons in SNI mice could alleviate anxiety- and depression-like behaviors and learning and memory impairment.
(A) Experimental schedule of virus injection and behavior tests. (B) Schematic of the coronal section of the mouse brain showed hM4Di virus injection. (C) AAV-CaMKIIα-hM4Di virus expressed in LH. Bar = 100 μm. (D) Merged confocal image of DAPI (Blue), hM4Di (Red) co-stained with CaMKIIα (Green) in LH slices. The white arrowheads indicate the colocalized cells that expressed both mCherry and CaMKIIα neurons. Scale bar, 100 μm. (E–F) The expression of c-Fos in LH decreased after injection of CNO. Scale bar, 100 μm. (mCherry: n = 3; hM4Di: n = 4. Unpaired student's t-test). (G) Mechanical PW threshold in the von Frey test (sham-mCherry: n = 9; sham-hM4Di: n = 11; SNI-mCherry: n = 10; SNI-hM4Di: n = 10. Two-way repeated measures ANOVA with Bonferroni's post hoc test). (H) Duration in the center in OFT (sham-mCherry: n = 9; sham-hM4Di: n = 11; SNI-mCherry: n = 9; SNI-hM4Di: n = 10, Two-way repeated measures ANOVA with Bonferroni's post hoc test). (I–J) EPM was performed. (I) Duration of exploring in the open arms (sham-mCherry: n = 9; sham-hM4Di: n = 9; SNI-mCherry: n = 9; SNI-hM4Di: n = 7. Two-way repeated measures ANOVA with Bonferroni's post hoc test). (J) The number of entering into the open arms (sham-mCherry: n = 9; sham-hM4Di: n = 9; SNI-mCherry: n = 9; SNI-hM4Di: n = 8. Two-way repeated measures ANOVA with Bonferroni's post hoc test). (K) The immobility time in the FST (sham-mCherry: n = 8; sham-hM4Di: n = 9; SNI-mCherry: n = 8; SNI-hM4Di: n = 8. Two-way repeated measures ANOVA with Bonferroni's post hoc test). (L) The latency to feed in an unfamiliar environment in NSF (sham-mCherry: n = 8; sham-hM4Di: n = 9; SNI-mCherry: n = 8; SNI-hM4Di: n = 7. Two-way repeated measures ANOVA with Bonferroni's post hoc test). (M) The grooming time in the SST (sham-mCherry: n = 8; sham-hM4Di: n = 9; SNI-mCherry: n = 8; SNI-hM4Di: n = 8. Two-way repeated measures ANOVA with Bonferroni's post hoc test). (N) SNI mice injected with hM4Di virus spent more time exploring in the novel arm in Y maze (sham-mCherry: n = 8; sham-hM4Di: n = 8; SNI-mCherry: n = 7; SNI-hM4Di: n = 7. Two-way repeated measures ANOVA with Bonferroni's post hoc test). (O–P) MWM was performed. (O) Escape latency in locating platform of the mice in the learning phase (sham-mCherry: n = 8; sham-hM4Di: n = 8; SNI-mCherry: n = 7; SNI-hM4Di: n = 7. Two-way repeated measures ANOVA with Bonferroni's post hoc test). (P) Duration in the target quadrant (sham-mCherry: n = 8; sham-hM4Di: n = 7; SNI-mCherry: n = 7; SNI-hM4Di: n = 7. Two-way repeated measures ANOVA with Bonferroni's post hoc test). Data were presented as the mean ± SEM. $^{*}P < 0.05$, $^{**}P < 0.01$, $^{***}P < 0.001$. (For interpretation of the references to color in this figure legend, the reader is referred to the Web version of this article.)

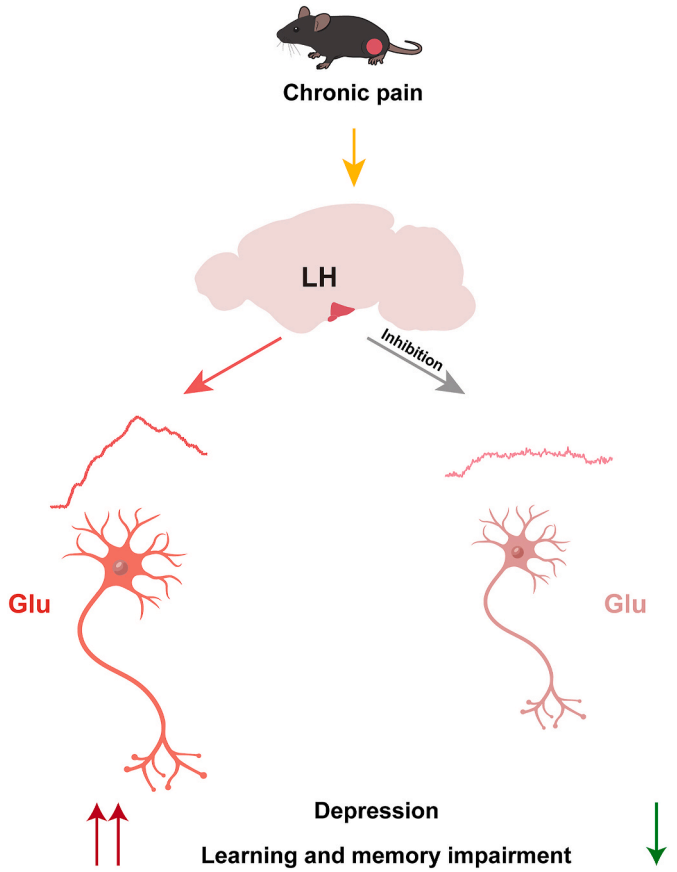

Fig. 6. Schematic diagram for LH glutamatergic neurons overactivation induced by chronic pain drives depression-like behaviors and learning and memory impairment. After SNI for 6 weeks, the activity of calcium signals in LH glutamatergic neurons increased, resulting in anxiety- and depression-like behaviors as well as learning and memory impairment. Inhibition of LH glutamatergic neurons in SNI mice alleviated anxiety- and depression-like behaviors as well as learning and memory impairment.

optogenetic activation of all glutamatergic neurons leads to an increase in both promoted and inhibited effects, ultimately resulting in no significant change in anxiety-like behavior. In contrast, SNI may specifically increase the excitability of the subpopulation of neurons that promote anxiety. Therefore, inhibiting all glutamatergic neurons in SNI mice, due to the suppression of the anxiety-promoting neuron subpopulation, while the excitability of the anxiety-inhibiting neurons remains at a lower level (unchanged), hence alleviated anxiety like behavior. To substantiate the plausibility of this hypothesis, we reviewed literature and found similar phenomena in other brain areas. For instance, the lateral septum (LS) and the central nucleus of the amygdala (CeA) represent two direct targets of the infralimbic cortex (IL), a subregion of the mPFC that modulates anxiety and fear. Surprisingly, these two projections were found to exert opposite effects on the anxious state: the IL-LS projection promoted anxiety-related behaviors, whereas the IL-CeA projection exerted anxiolytic effects on the same features (Chen et al., 2021).

Glutamatergic neurons in LH also can be divided into several subpopulations, distinguished by their expression of neuropeptides, projected targets, or received inputs, that may play different roles in the behaviors. For instance, three major subpopulations can be identified based on the expression of neuropeptides: hypocretin/orexin (Hcrt/Ox), melanin-concentrating hormone (MCH), and a mixed population express various neuropeptide and receptor markers. Importantly, activation of orexinergic neurons and galanin neurons in LH relieves anxiety-like behavior induced by chronic social defeat stress (Eghtesad et al., 2022; Owens-French et al., 2022; Wang et al., 2021). Secondly, the LH receives extensive projections from upstream brain regions and can project onto many downstream brain regions that play different roles in modulating anxiety-like behavior. Optogenetic activation of the vCA1 terminals in the LH increases anxiety-like behavior (Jimenez et al., 2018), whereas inhibiting LH-projecting BNST neurons induces anxiety-like behavior (Yamauchi et al., 2022). Therefore, the mechanisms upstream and downstream of the LH and the neuronal subtypes involved in SNI-induced anxiety, depression, and cognitive impairments require further clarification.

In addition, there is one more point that needs our attention, only male mice were included in our study. It has been reported that sex-specific differences are pronounced under neuropathic pain conditions and may be influenced by multiple factors. The impact of chronic pain on anxiety, depression, and cognition in female mice, along with the underlying mechanisms, requires further investigation.

In conclusion, we identified that chronic pain causes anxiety- and depression-like behaviors and learning and memory impairment, and strong activation of glutamatergic neurons in the LH. We adopted chemogenetic and optogenetic methods to enhance LH activation and found that the mice showed some of the depression-like behavior, and learning and memory impairment. Inhibition of LH activation in SNI mice alleviates anxiety- and depression-like behaviors and learning and memory impairment. Our study offers preliminary insights into the potential mechanisms by which chronic pain may influence certain anxiety- and depression-like behaviors, as well as aspects of learning and memory impairment.

Funding

This work was supported by the National Natural Science Foundation of China (No. 32200832, No. 82001207, No. 81771144), Guangdong Basic and Applied Basic Research Foundation (No. 2024A15150111398, No. 2022A1515012553) The Research Foundation of Medical Science and Technology of Guangdong Province (No. A2022262).

CRediT authorship contribution statement

Lianghui Meng: Writing – original draft, Data curation. **Xuefeng Zheng:** Writing – review & editing, Writing – original draft, Investigation. **Keman Xie:** Software, Resources. **Yifei Li:** Formal analysis, Data curation. **Danlei Liu:** Visualization, Resources. **Yuanyuan Xu:** Methodology, Formal analysis. **Jifeng Zhang:** Writing – review & editing, Investigation, Data curation. **Fengming Wu:** Writing – review & editing, Writing – original draft. **Guoqing Guo:** Writing – review & editing, Writing – original draft, Funding acquisition.

Declaration of competing interest

The authors declare no conflict of interest.

Data availability

Data will be made available on request.

Acknowledgements

Not applicable.

Appendix A. Supplementary data

Supplementary data to this article can be found online at https://doi.org/10.1016/j.ynstr.2024.100654.

References

Bonilla-Jaime, H., Sánchez-Salcedo, J.A., Estevez-Cabrera, M.M., Molina-Jiménez, T., Cortes-Altamirano, J.L., Alfaro-Rodríguez, A., 2022. Depression and pain: use of antidepressants. Curr. Neuropharmacol. 20 (2), 384–402.

Bonnavion, P., Mickelsen, L.E., Fujita, A., de Lecea, L., Jackson, A.C., 2016. Hubs and spokes of the lateral hypothalamus: cell types, circuits and behaviour. J Physiol. 594 (22), 6443–6462.

Burdakov, D., Peleg-Raibstein, D., 2020. The hypothalamus as a primary coordinator of memory updating. Physiol. Behav. 223, 112988.

Chen, T., Wang, J., Wang, Y.Q., Chu, Y.X., 2022. Current understanding of the neural circuitry in the comorbidity of chronic pain and anxiety. Neural Plast. 2022, 4217593.

Chen, Y.H., Wu, J.L., Hu, N.Y., Zhuang, J.P., Li, W.P., Zhang, S.R., Li, X.W., Yang, J.M., Gao, T.M., 2021. Distinct projections from the infralimbic cortex exert opposing effects in modulating anxiety and fear. J. Clin. Invest. 131 (14), e145692.

Cryan, J.F., Mombereau, C., Vassout, A., 2005. The tail suspension test as a model for assessing antidepressant activity: review of pharmacological and genetic studies in mice. Neurosci. Biobehav. Rev. 29 (4–5), 571–625.

Cui, Y., Huang, X., Huang, P., Huang, L., Feng, Z., Xiang, X., Chen, X., Li, A., Ren, C., Li, H., 2022. Reward ameliorates depressive-like behaviors via inhibition of the substantia innominata to the lateral habenula projection. Sci. Adv. 8 (27), eabn0193.

Dai, W., Huang, S., Luo, Y., Cheng, X., Xia, P., Yang, M., Zhao, P., Zhang, Y., Lin, W.J., Ye, X., 2022. Sex-specific transcriptomic signatures in brain regions critical for neuropathic pain-induced depression. Front. Mol. Neurosci. 15, 886916.

Davis, K.D., Flor, H., Greely, H.T., Iannetti, G.D., Mackey, S., Ploner, M., Pustilnik, A., Tracey, I., Treede, R.D., Wager, T.D., 2017. Brain imaging tests for chronic pain: medical, legal and ethical issues and recommendations. Nat. Rev. Neurol. 13 (10), 624–638.

Davis, K.D., Moayedi, M., 2013. Central mechanisms of pain revealed through functional and structural MRI. J. Neuroimmune Pharmacol. 8 (3), 518–534.

Daviu, N., Füzesi, T., Rosenegger, D.G., Rasiah, N.P., Sterley, T.L., Peringod, G., Bains, J. S., 2020. Paraventricular nucleus CRH neurons encode stress controllability and regulate defensive behavior selection. Nat. Neurosci. 23 (3), 398–410.

Decosterd, I., Woolf, C.J., 2000. Spared nerve injury: an animal model of persistent peripheral neuropathic pain. Pain 87 (2), 149–158.

Donnelly, C.R., Chen, O., Ji, R.R., 2020. How do sensory neurons sense danger signals? Trends Neurosci. 43 (10), 822–838.

Eghtesad, M., Elahdadi, S.M., Lashkarbolouki, T., Goudarzi, I., 2022. Lateral hypothalamus corticotropin-releasing hormone receptor-1 inhibition and modulating stress-induced anxiety behavior. Basic Clin. Neurosci. 13 (3), 373–384.

Ferrario, C.R., Finnell, J.E., 2023. Beyond the hypothalamus: roles for insulin as a regulator of neurotransmission, motivation, and feeding. Neuropsychopharmacology 48 (1), 232–233.

Floresco, S.B., 2015. The nucleus accumbens: an interface between cognition, emotion, and action. Annu. Rev. Psychol. 66, 25–52.

Gilam, G., Gross, J.J., Wager, T.D., Keefe, F.J., Mackey, S.C., 2020. What is the relationship between pain and emotion? Bridging constructs and communities. Neuron 107 (1), 17–21.

Gu, H., Zhang, G., Liu, P., Pan, W., Tao, Y., Zhou, Z., Yang, J., 2023. Contribution of activating lateral hypothalamus-lateral habenula circuit to nerve trauma-induced neuropathic pain in mice. Neurobiol. Dis. 182, 106155-106155.

Hao, Y., Ge, H., Sun, M., Gao, Y., 2019. Selecting an appropriate animal model of depression. Int. J. Mol. Sci. 20 (19).

Hashmi, J.A., Baliki, M.N., Huang, L., Baria, A.T., Torbey, S., Hermann, K.M., Schnitzer, T.J., Apkarian, A.V., 2013. Shape shifting pain: chronification of back pain shifts brain representation from nociceptive to emotional circuits. Brain 136 (Pt 9), 2751–2768.

Hu, R.K., Zuo, Y., Ly, T., Wang, J., Meera, P., Wu, Y.E., Hong, W., 2021. An amygdala-to-hypothalamus circuit for social reward. Nat. Neurosci. 24 (6), 831–842.

Jennings, J.H., Rizzi, G., Stamatakis, A.M., Ung, R.L., Stuber, G.D., 2013. The inhibitory circuit architecture of the lateral hypothalamus orchestrates feeding. Science 341 (6153), 1517–1521.

Jia, X., Chen, S., Li, X., Tao, S., Lai, J., Liu, H., Huang, K., Tian, Y., Wei, P., Yang, F., Lu, Z., Chen, Z., Liu, X.A., Xu, F., Wang, L., 2022. Divergent neurocircuitry dissociates two components of the stress response: glucose mobilization and anxiety-like behavior. Cell Rep. 41 (6), 111586.

Jimenez, J.C., Su, K., Goldberg, A.R., Luna, V.M., Biane, J.S., Ordek, G., Zhou, P., Ong, S. K., Wright, M.A., Zweifel, L., Paninski, L., Hen, R., Kheirbek, M.A., 2018. Anxiety cells in a hippocampal-hypothalamic circuit. Neuron 97 (3), 670–683.e6.

Kelly, C.J., Huang, M., Meltzer, H., Martina, M., 2016. Reduced glutamatergic currents and dendritic branching of layer 5 pyramidal cells contribute to medial prefrontal cortex deactivation in a rat model of neuropathic pain. Front. Cell. Neurosci. 10, 133.

Kraeuter, A.K., Guest, P.C., Sarnyai, Z., 2019a. The open field test for measuring locomotor activity and anxiety-like behavior. Methods Mol. Biol. 1916, 99–103.

Kraeuter, A.K., Guest, P.C., Sarnyai, Z., 2019b. The elevated plus maze test for measuring anxiety-like behavior in rodents. Methods Mol. Biol. 1916, 69–74.

Kraeuter, A.K., Guest, P.C., Sarnyai, Z., 2019c. The Y-maze for assessment of spatial working and reference memory in mice. Methods Mol. Biol. 1916, 105–111.

Kremer, M., Becker, L.J., Barrot, M., Yalcin, I., 2021. How to study anxiety and depression in rodent models of chronic pain? Eur. J. Neurosci. 53 (1), 236–270.

Kroenke, K.M.D., Outcalt, S.P.D., Krebs, E.M.D., Bair, M.J.M.D., Wu, J.M.S., Chumbler, N.P.D., Yu, Z.P.D., 2013. Association between anxiety, health-related quality of life and functional impairment in primary care patients with chronic pain. Gen. Hosp. Psychiatr. 35 (4), 359–365.

Lazaridis, I., Tzortzi, O., Weglage, M., Martin, A., Xuan, Y., Parent, M., Johansson, Y., Fuzik, J., Furth, D., Fenno, L.E., Ramakrishnan, C., Silberberg, G., Deisseroth, K., Carlen, M., Meletis, K., 2019. A hypothalamus-habenula circuit controls aversion. Mol Psychiatry 24 (9), 1351–1368.

Li, Y.D., Luo, Y.J., Chen, Z.K., Quintanilla, L., Cherasse, Y., Zhang, L., Lazarus, M., Huang, Z.L., Song, J., 2022. Hypothalamic modulation of adult hippocampal neurogenesis in mice confers activity-dependent regulation of memory and anxiety-like behavior. Nat. Neurosci. 25 (5), 630–645.

Li, Y., Li, Y., Zhang, X., Li, Y., Liu, Y., Xu, H., 2023. CaMKIIa neurons of the ventromedial hypothalamus mediate wakefulness and anxiety-like behavior. Neurochem. Res.

Li, Y., Ritzel, R.M., Khan, N., Cao, T., He, J., Lei, Z., Matyas, J.J., Sabirzhanov, B., Liu, S., Li, H., Stoica, B.A., Loane, D.J., Faden, A.I., Wu, J., 2020. Delayed microglial depletion after spinal cord injury reduces chronic inflammation and neurodegeneration in the brain and improves neurological recovery in male mice. Theranostics 10 (25), 11376–11403.

Ma, Y., Xiang, Q., Yan, C., Liao, H., Wang, J., 2021. Relationship between chronic diseases and depression: the mediating effect of pain. BMC Psychiatr. 21 (1), 436.

Mayer, E.A., Gupta, A., Kilpatrick, L.A., Hong, J.Y., 2015. Imaging brain mechanisms in chronic visceral pain. Pain 156 (Suppl. 1), S50–S63 (0 1).

Morasco, B.J., Lovejoy, T.I., Lu, M., Turk, D.C., Lewis, L., Dobscha, S.K., 2013. The relationship between PTSD and chronic pain: mediating role of coping strategies and depression. Pain 154 (4), 609–616.

Narita, M., Kuzumaki, N., Narita, M., Kaneko, C., Hareyama, N., Miyatake, M., Shindo, K., Miyoshi, K., Nakajima, M., Nagumo, Y., Sato, F., Wachi, H., Seyama, Y., Suzuki, T., 2006. Chronic pain-induced emotional dysfunction is associated with astrogliosis due to cortical delta-opioid receptor dysfunction. J. Neurochem. 97 (5), 1369–1378.

Othman, M.Z., Hassan, Z., Che, H.A., 2022. Morris water maze: a versatile and pertinent tool for assessing spatial learning and memory. Exp. Anim. 71 (3), 264–280.

Otis, J.M., Zhu, M., Namboodiri, V., Cook, C.A., Kosyk, O., Matan, A.M., Ying, R., Hashikawa, Y., Hashikawa, K., Trujillo-Pisanty, I., Guo, J., Ung, R.L., Rodriguez-Romaguera, J., Anton, E.S., Stuber, G.D., 2019. Paraventricular thalamus projection neurons integrate cortical and hypothalamic signals for cue-reward processing. Neuron 103 (3), 423–431.e4.

Owens-French, J., Li, S.B., Francois, M., Leigh, T.R., Daniel, M., Soulier, H., Turner, A., de Lecea, L., Münzberg, H., Morrison, C., Qualls-Creekmore, E., 2022. Lateral hypothalamic galanin neurons are activated by stress and blunt anxiety-like behavior in mice. Behav. Brain Res. 423, 113773.

Rayner, L., Hotopf, M., Petkova, H., Matcham, F., Simpson, A., Mccracken, L.M., 2016. Depression in patients with chronic pain attending a specialised pain treatment centre: prevalence and impact on health care costs. Pain 157 (7), 1472–1479.
Schindler, S, Schmidt, L, Stroske, M, Storch, M, Anwander, A, Trampel, R, Strauss, M, Hegerl, U, Geyer, S, Schonknecht, P, 2019. Hypothalamus enlargement in mood disorders. Acta Psychiatr Scand 139 (1), 56–67.
Schwartz, N., Temkin, P., Jurado, S., Lim, B.K., Heifets, B.D., Polepalli, J.S., Malenka, R. C., 2014. Chronic pain. Decreased motivation during chronic pain requires long-term depression in the nucleus accumbens. Science 345 (6196), 535–542.
Sharpe, M.J., Marchant, N.J., Whitaker, L.R., Richie, C.T., Zhang, Y.J., Campbell, E.J., Koivula, P.P., Necarsulmer, J.C., Mejias-Aponte, C., Morales, M., Pickel, J., Smith, J. C., Niv, Y., Shaham, Y., Harvey, B.K., Schoenbaum, G., 2017. Lateral hypothalamic GABAergic neurons encode reward predictions that are relayed to the ventral tegmental area to regulate learning. Curr. Biol. 27 (14), 2089–2100.e5.
Shin, A., Ryoo, J., Shin, K., Lee, J., Bae, S., Kim, D.G., Park, S.G., Kim, D., 2023. Exploration driven by a medial preoptic circuit facilitates fear extinction in mice. Commun. Biol. 6 (1), 106.
Sprenger, T, Valet, M, Platzer, S, Pfaffenrath, V, Steude, U, Tolle, T R, 2005. SUNCT: bilateral hypothalamic activation during headache attacks and resolving of symptoms after trigeminal decompression. Pain 113 (3), 422–426.
Tang, H.D., Dong, W.Y., Hu, R., Huang, J.Y., Huang, Z.H., Xiong, W., Xue, T., Liu, J., Yu, J.M., Zhu, X., Zhang, Z., 2022. A neural circuit for the suppression of feeding under persistent pain. Nat. Metab. 4 (12), 1746–1755.
Tappe-Theodor, A., Kuner, R., 2019. A common ground for pain and depression. Nat. Neurosci. 22 (10), 1612–1614.
Tran, L.T., Park, S., Kim, S.K., Lee, J.S., Kim, K.W., Kwon, O., 2022. Hypothalamic control of energy expenditure and thermogenesis. Exp. Mol. Med. 54 (4), 358–369.
Wang, D., Li, A., Dong, K., Li, H., Guo, Y., Zhang, X., Cai, M., Li, H., Zhao, G., Yang, Q., 2021. Lateral hypothalamus orexinergic inputs to lateral habenula modulate maladaptation after social defeat stress. Neurobiol Stress 14, 100298.
Wang, D., Pan, X., Zhou, Y., Wu, Z., Ren, K., Liu, H., Huang, C., Yu, Y., He, T., Zhang, X., Yang, L., Zhang, H., Han, M., Liu, C., Cao, J., Yang, C., 2023. Lateral septum-lateral hypothalamus circuit dysfunction in comorbid pain and anxiety. Mol. Psychiatr. 28 (3), 1090–1100.
Wang, M., Li, P., Li, Z., Da, S.B., Zheng, W., Xiang, Z., He, Y., Xu, T., Cordeiro, C., Deng, L., Dai, Y., Ye, M., Lin, Z., Zhou, J., Zhou, X., Ye, F., Cunha, R.A., Chen, J., Guo, W., 2023. Lateral septum adenosine A(2A) receptors control stress-induced depressive-like behaviors via signaling to the hypothalamus and habenula. Nat. Commun. 14 (1), 1880.
Wang, Y., Shi, Y., Huang, Y., Liu, W., Cai, G., Huang, S., Zeng, Y., Ren, S., Zhan, H., Wu, W., 2020. Resveratrol mediates mechanical allodynia through modulating inflammatory response via the TREM2-autophagy axis in SNI rat model. J. Neuroinflammation 17 (1), 311.
Willner, P., Towell, A., Sampson, D., Sophokleous, S., Muscat, R., 1987. Reduction of sucrose preference by chronic unpredictable mild stress, and its restoration by a tricyclic antidepressant. Psychopharmacology (Berl). 93 (3), 358–364.
Yamauchi, N., Sato, K., Sato, K., Murakawa, S., Hamasaki, Y., Nomura, H., Amano, T., Minami, M., 2022. Chronic pain-induced neuronal plasticity in the bed nucleus of the stria terminalis causes maladaptive anxiety. Sci. Adv. 8 (17), eabj5586.
Yan, J., Ding, X., He, T., Chen, A., Zhang, W., Yu, Z., Cheng, X., Wei, C., Hu, Q., Liu, X., Zhang, Y., He, M., Xie, Z., Zha, X., Xu, C., Cao, P., Li, H., Xu, X., 2022. A circuit from the ventral subiculum to anterior hypothalamic nucleus GABAergic neurons essential for anxiety-like behavioral avoidance. Nat. Commun. 13 (1), 7464-7464.
Yankelevitch-Yahav, R., Franko, M., Huly, A., Doron, R., 2015. The forced swim test as a model of depressive-like behavior. J. Vis. Exp. 97.
Zhang, J.F., Williams, J.P., Shi, W.R., Qian, X.Y., Zhao, Q.N., Lu, G.F., An, J.X., 2022. Potential molecular mechanisms of electroacupuncture with spatial learning and memory impairment induced by chronic pain on a rat model. Pain Physician 25 (2), E271–E283.
Zhang, X., Gao, R., Zhang, C., Chen, H., Wang, R., Zhao, Q., Zhu, T., Chen, C., 2021. Evidence for cognitive decline in chronic pain: a systematic review and meta-analysis. Front. Neurosci. 15, 737874.
Zheng, Z., Guo, C., Li, M., Yang, L., Liu, P., Zhang, X., Liu, Y., Guo, X., Cao, S., Dong, Y., Zhang, C., Chen, M., Xu, J., Hu, H., Cui, Y., 2022. Hypothalamus-habenula potentiation encodes chronic stress experience and drives depression onset. Neuron 110 (8), 1400–1415.e6.
Zhou, W., Jin, Y., Meng, Q., Zhu, X., Bai, T., Tian, Y., Mao, Y., Wang, L., Xie, W., Zhong, H., Zhang, N., Luo, M.H., Tao, W., Wang, H., Li, J., Li, J., Qiu, B.S., Zhou, J. N., Li, X., Xu, H., Wang, K., Zhang, X., Liu, Y., Richter-Levin, G., Xu, L., Zhang, Z., 2019. A neural circuit for comorbid depressive symptoms in chronic pain. Nat. Neurosci. 22 (10), 1649–1658.
Zhou, X., Risold, P., Alvarez-Bolado, G., 2021. Development of the GABAergic and glutamatergic neurons of the lateral hypothalamus. J. Chem. Neuroanat. 116, 101997-101997.
Zinsmaier, A.K., Dong, Y., Huang, Y.H., 2022. Cocaine-induced projection-specific and cell type-specific adaptations in the nucleus accumbens. Mol Psychiatry 27 (1), 669–686.